Arteriosclerosis, Thrombosis, and Vascular Biology
JOURNAL OF THE AMERICAN HEART ASSOCIATION

Hepcidin Destabilizes Atherosclerotic Plaque Via Overactivating Macrophages After Erythrophagocytosis

Jing Jing Li, Xiao Meng, Hai Peng Si, Cheng Zhang, Hui Xia Lv, Yu Xia Zhao, Jian Min Yang, Mei Dong, Kai Zhang, Su Xia Liu, Xue Qiang Zhao, Fei Gao, Xiao Ling Liu, Tai Xing Cui and Yun Zhang

Arterioscler Thromb Vasc Biol 2012, 32:1158-1166: originally published online March 1, 2012
doi: 10.1161/ATVBAHA.112.246108
Arteriosclerosis, Thrombosis, and Vascular Biology is published by the American Heart Association. 7272 Greenville Avenue, Dallas, TX 72514
 Print ISSN: 1079-5642. Online ISSN: 1524-4636

Hepcidin Destabilizes Atherosclerotic Plaque Via Overactivating Macrophages After Erythrophagocytosis

Jing Jing Li,* Xiao Meng,* Hai Peng Si, Cheng Zhang, Hui Xia Lv, Yu Xia Zhao, Jian Min Yang, Mei Dong, Kai Zhang, Su Xia Liu, Xue Qiang Zhao, Fei Gao, Xiao Ling Liu, Tai Xing Cui, Yun Zhang

Objective—To explore a direct and causal relationship between vascular hepcidin and atherosclerotic plaque stability.

Methods and Results—Accelerated atherosclerotic lesions were established by perivascular collar placement in apolipoprotein E–deficient ($ApoE^{-/-}$) mice. Adenoviral overexpression of hepcidin in the carotid artery during plaque formation enhanced intraplaque macrophage infiltration and suppressed the contents of collagen and vascular smooth muscle cells, whereas hepcidin shRNA treatment exerts opposite effects. The overexpression or knockdown of hepcidin did not affect plaque lipid deposition but increased or decreased oxidized low-density lipoprotein (ox-LDL) levels within intraplaque macrophages. In cultured macrophages, ox-LDL not only increased reactive oxygen species formation, inflammatory cytokine production, and apoptosis but also upregulated hepcidin expression. However, hepcidin did not exaggerate the ox-LDL–induced activation of macrophages until an onset of erythrophagocytosis. Whereas hepcidin was critical for the upregulation of L-ferritin and H-ferritin in both ox-LDL–treated erythrophagocytosed macrophages and atherosclerotic plaques, the adding of iron chelators suppressed the intracellular lipid accumulation, reactive oxygen species formation, inflammatory cytokine expression, and apoptosis in erythrophagocytosed macrophages.

Conclusion—Hepcidin promotes plaque destabilization partly by exaggerating inflammatory cytokine release, intracellular lipid accumulation, oxidative stress, and apoptosis in the macrophages with iron retention. **(*Arterioscler Thromb Vasc Biol*. 2012;32:1158-1166.)**

Key Words: atherosclerosis ■ macrophages ■ erythrophagocytosis ■ hepcidin ■ plaque stability

It has been documented for decades that a state of sustained iron depletion or mild iron deficiency protects against atherosclerosis.[1] Although a few risk factors for cardiovascular disease including overactivation of the renin-angiotensin system and polymorphisms of haptoglobin or heme oxygenase promoter are associated with increased atherosclerotic plaque iron,[1] an approach of iron depletion either delays the onset of atherogenesis or stabilizes plaque.[2] Importantly, the storage and processing of iron from erythrophagocytosis by macrophages within plaque appear to play a key role in plaque progression. Accordingly, we have demonstrated that erythrocytes induce plaque vulnerability in a dose-dependent manner in a rabbit model of intraplaque hemorrhage.[3] However, a plausible link between the retention of iron in macrophages and atherosclerotic lesion formation and development remains unknown.

Recently, hepcidin has been demonstrated to be a key peptide in the regulation of iron homeostasis.[4,5] Hepcidin binds to the iron transporter Ferroportin 1 (FPN1) on the cell surface and induces FPN1 internalization and degradation.[6] As a result, the intracellular iron level is elevated. Hepcidin is produced by a wide variety of cells including macrophages,[5] and the expression of hepcidin is regulated by a number of factors. For instance, hepcidin expression is increased in response to iron supplement and inflammation and decreased in response to iron insufficiency.[6] Notably, hepcidin is a major determinant of the amount of iron retained in macrophages.[7] Therefore, it has been suggested that hepcidin promotes atherosclerosis progression by slowing or preventing the mobilization of iron from macrophages within the atherosclerotic lesion.[8] Valenti et al[9] found that the serum hepcidin and macrophage iron levels correlated with MCP-1

Received on: August 26, 2011; final version accepted on: February 13, 2012.

From the Key Laboratory of Cardiovascular Remodeling and Function Research, Chinese Ministry of Education and Chinese Ministry of Health, Shandong University, Jinan, Shandong, China (J.J.L., X.M., C.Z., H.X.L., Y.X.Z., J.M.Y., M.D., K.Z., S.X.L., X.Q.Z., F.G., X.L.L., Y.Z.); the Department of Orthopedics, Second Hospital, Shandong University, Jinan, Shandong, China (H.P.S.); and the Department of Cell Biology and Anatomy, University of South Carolina School of Medicine, Columbia, SC (T.X.C.).

*J.J.L. and X.M. contributed equally to this work.

The online-only Data Supplement is available with this article at http://atvb.ahajournals.org/lookup/suppl/doi:10.1161/ATVBAHA.112.246108/-/DC1.

Correspondence to Yun Zhang, MD, PhD, FACC, Qilu Hospital, Shandong University No.107, Wen Hua Xi Road, Jinan, Shandong, 250012, PR China. E-mail zhangyun@sdu.edu.cn; or Tai Xing Cui, MD, PhD, Department of Cell Biology and Anatomy, University of South Carolina School of Medicine, Columbia, SC 29208. E-mail Taixing.Cui@uscmed.sc.edu

release and vascular damage in patients with metabolic syndrome. More recently, Saeed et al[10] showed that reduction of the iron levels of macrophages via systemic pharmacological suppression of hepcidin increased expression of cholesterol efflux transporters and attenuated atherosclerosis. Nevertheless, a direct and causal relationship between vascular hepcidin and atherosclerotic plaque stability and the potential mechanisms have not yet been explored.

In the present study, we studied the potential role of vascular hepcidin in atherosclerotic plaque stability by local hepcidin gain- and loss-of-function approaches in a mouse model of accelerated atherosclerosis and explored the underlying mechanisms in macrophages under a proatherogenic microenvironment.

Methods

Detailed material and methods are described in the online-only Data Supplement.

Preparation of Adenoviral Vectors

Recombinant adenoviruses (Ad) carrying the murine hepcidin (Ad-hepcidin) and its shRNA or a control transgene EGFP (Ad-EGFP) were prepared.

Animal Model and Gene Transfer

In the first part of the in vivo study, 40 male apolipoprotein E (apoE)$^{-/-}$ mice were randomly divided into a control group and a model group (n=20 each). Mice in the model group underwent constrictive collar placement around the left common carotid artery near its bifurcation as previously described.[11] In the second part of the in vivo study, 75 male apoE$^{-/-}$ mice underwent constrictive collar placement and were randomly divided into 3 groups (n=25 each) for adenoviral gene delivery of Ad-EGFP, Ad-hepcidin, and Ad-hepcidin shRNA, respectively.

Serum Lipid, Glucose, and Iron Measurement

At the end of the second part of the in vivo study, serum total cholesterol (TC), triglycerides (TG), low-density lipoprotein (LDL-C) cholesterol, and high-density lipoprotein cholesterol (HDL) and glucose concentrations were measured.

Tissue Preparation and Histological Analysis

Antihepcidin monoclonal antibody (1:150, Abcam, Cambridge, United Kingdom) was used for hepcidin staining in vivo. Positive staining areas of macrophages, smooth muscle cells (SMCs), lipids, collagen, IL-6, MCP-1, TNFα, MMP-2, hepcidin, H-ferritin, and L-ferritin were quantified. The vulnerable index was calculated as described in previous studies.[12]

Immunofluorescence

Tissue sections of the carotid arteries were incubated with double primary antibodies, including those against macrophages and hepcidin, SMCs and hepcidin, macrophages, and oxidized LDL (ox-LDL) as well as SMCs and ox-LDL. Fluorescent images were obtained by a laser scanning confocal microscopy.

Cell Culture and Treatment

J774 macrophages were chosen for erythrophagocytosis as previously described.[13] Monolayers of J774 macrophages with or without erythrophagocytosis were treated with ox-LDL, synthetic human hepcidin, desferrioxamine (DFO), and ferrous chelator 2,2′-bipyridyl (BPDL).[14,15] Monolayers of J774 macrophages transfected with control or hepcidin siRNAs were subjected to erythrophagocytosis and given different treatments.

Quantitative Real-Time PCR

The mRNA expression levels of hepcidin, IL-6, MCP-1, TNFα, MMP-2, FPN1, H-ferritin, and L-ferritin were quantified.

Western Blot Analysis

The protein expression levels of IL-6, MCP-1, TNFα, H-ferritin, and L-ferritin were quantitatively analyzed.

Immunocytochemistry

Antihepcidin monoclonal antibodies (1:100, Abcam) were applied for immunofluorescent staining of hepcidin. Expression and localization of hepcidin and FPN1 in J774 macrophages were examined.

Quantification of Reactive Oxygen Species Production

Fluorescence measurement of reactive oxygen species (ROS) was performed with Flow Cytometer, and the data were analyzed with Cell Quest Pro.

Detection of Apoptosis

Apoptosis was assessed by terminal deoxynucleotidyl transferase end-labeling staining (TUNEL).

ELISA

The concentrations of hepcidin in serum and supernatant were determined by ELISA.

Quantification of Intracellular Lipids

The lipids of macrophages with different treatments were extracted with the Folch method, and the intracellular TC, TG, and LDL-C were measured by enzymatic assay.

Measurement of Nonheme Iron by Atomic Absorption Spectrometry

The levels of nonheme iron in atherosclerotic plaques were measured by flame atomic absorption spectrometry.

Statistical Analysis

The data are expressed as mean±SEM. An independent-samples *t* test was used to compare continuous data for between-group differences, and comparisons among groups involved the use of ANOVA with least-squares difference post hoc test used for multiple comparisons. $P<0.05$ was considered statistically significant.

Results

Upregulation of Hepcidin Expression in Atherosclerotic Plaques

To clarify the role of hepcidin in atherogenesis, we first examined hepcidin expression in the carotid plaques in ApoE$^{-/-}$ mice. Relative to the homolateral carotid arteries in the control group without atherosclerotic lesions, both mRNA and protein expression levels of hepcidin were upregulated in the carotid plaques (Figure IA– IC in the online-only Data Supplement). These findings indicated a potential role of vascular hepcidin in the pathogenesis of atherosclerosis.[9]

Critical Role of Hepcidin in Plaque Instability and Inflammation

Second, we applied local hepcidin gain- and loss-of-function approaches by adenoviral delivery of hepcidin and its shRNA into the atherosclerotic carotid arteries to address a precise role of vascular hepcidin in plaque stability. Because GFP provides a convenient monitor for checking the efficiency of adenovirus infection, the GFP fluorescence in the carotid

plaques infected with Ad-EGFP, Ad-EGFP-hepcidin (Ad-hepcidin), and Ad-EGFP-hepcidin shRNA (Ad-hepcidin shRNA) was examined. Elevated and comparable levels of fluorescent densities were observed in plaques of these infected carotid arteries, appearing at 1 week after infection and sustaining for additional 2 weeks. In our preliminary study, we measured the ratio of the GFP-positive staining area to the plaque area in the 3 treatment groups of mice 2 weeks after the infection, and the ratio was 0.67±0.15, 0.68±0.08, and 0.64±0.17 in the Ad-EGFP, Ad-hepcidin, and Ad-hepcidin shRNA groups, respectively ($P>0.05$), which demonstrates a similar infection efficiency among these 3 groups. At the end of the experiment, hepcidin expression in the carotid arteries was upregulated in the Ad-hepcidine group but downregulated in the Ad-hepcidin shRNA group (Figure 1A through 1C). To further characterize the intraplaque cell types of hepcidin overexpression, we double-stained hepcidin and macrophages or SMCs of atherosclerotic carotid plaques transfected with Ad-hepcidin and found that the local hepcidin gain-of-function approach led to an increase of hepcidin expression in intraplaque macrophages and SMCs (Figure 1D). In contrast, the manipulation of hepcidin expression hardly affected the serum lipid and glucose levels (Table in the online-only Data Supplement). There was no significant difference of serum hepcidin and hepatic hepcidin mRNA levels among the 3 groups of mice (Figure 1E and 1F).

It is worth noting that neither the overexpression nor knockdown of hepcidin altered the plaque size, relative to the control (Figure 2B). However, the plaque composition including macrophages, SMCs, and collagen was significantly affected by the hepcidin overexpression or knockdown. The hepcidin overexpression increased intraplaque macrophages and decreased intraplaque SMCs, whereas hepcidin knockdown exerted opposite effects (Figure 2A and 2D). There was no significant difference of total lipid levels in the plaques among the Ad-EGFP, Ad-hepcidin, and Ad-hepcidin shRNA groups (Figure 2A and 2D). It is interesting that the expression level of ox-LDL in intraplaque macrophages was substantially enhanced by hepcidin overexpression but was dramatically suppressed by hepcidin knockdown (Figure 2G and 2H). Accordingly, the plaque vulnerability index was elevated by the hepcidin overexpression but reduced by the hepcidin knockdown, respectively (Figure 2C), which suggests that hepcidin plays a critical role in plaque destabilization.

Considering a crucial role of inflammation in the pathogenesis of atherosclerosis,[16] we further examined whether hepcidin overexpression or knockdown regulates vascular inflammatory responses in the atherosclerotic lesions. The results showed that the expression levels of IL-6, MCP-1, TNFα, and MMP-2 were substantially enhanced by hepcidin overexpression but were dramatically suppressed by hepcidin knockdown (Figure 2A, 2E, and 2F), which suggests that hepcidin destabilizes atherosclerotic plaques at least partly by exaggerating inflammatory responses in atherosclerotic lesions.

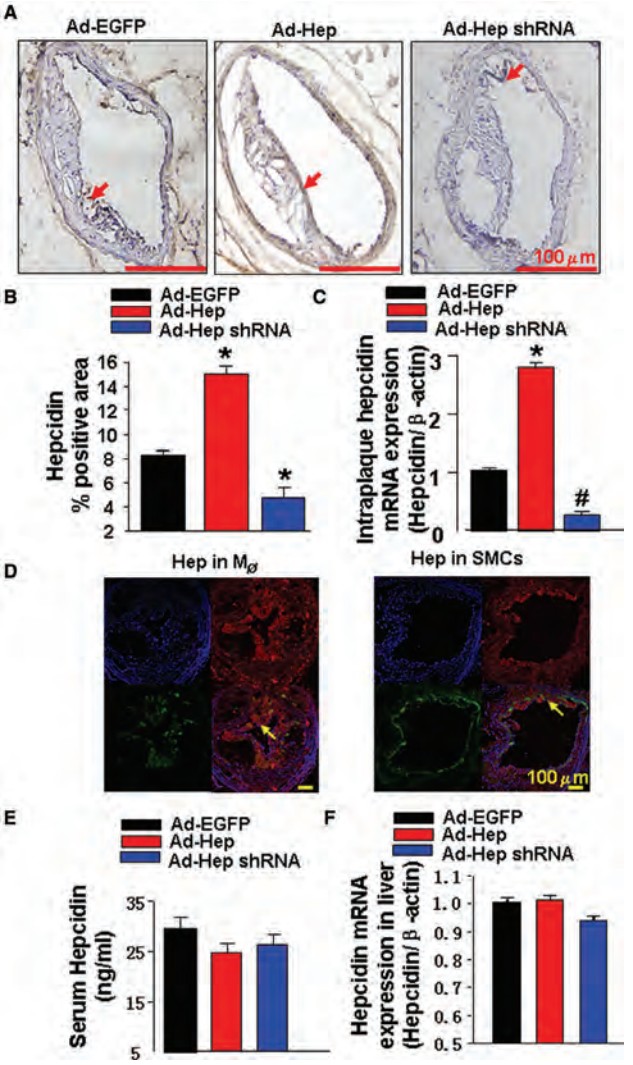

Figure 1. Expression of hepcidin in 3 groups of mice. **A**, Immunochemical staining of hepcidin in the carotid plaques of the 3 treatment groups. **Arrowheads** indicate positive staining areas in brown. Hep indicates Hepcidin. **B**, Quantitative analysis of the results in **A** (n=6 in each group). *$P<0.01$ versus Ad-EGFP group. **C**, Hepcidin mRNA expression in the carotid plaques of the 3 treatment groups; 4 polls in each group and 3 arteries as a poll. *$P<0.01$ versus Ad-EGFP group, #$P<0.05$ versus Ad-EGFP group. **D**, Cells expressing hepcidin in a plaque of the Ad-hepcidin group. In the **left panel**, blue color indicates macrophage nuclei; red color displays hepcidin; green color depicts macrophages; double red and green staining signifies the expression of hepcidin in macrophages. In the **right panel**, blue color indicates SMCs nuclei; red color displays hepcidin; green color depicts SMCs; double staining of red and green signifies the expression of hepcidin in SMCs. **Arrowheads** indicate positive staining areas. $M_ø$ indicates macrophages. **E**, Serum hepcidin levels of the 3 treatment groups quantified by ELISA (n=6 in each group). **F**, Hepcidin mRNA expression in the livers of the 3 treatment groups (n=6 in each group).

Essential Role of Hepcidin in ox-LDL–mediated Phenotypic Modulation of Macrophages After Erythrophagocytosis

Because of the potential link of hepcidin, macrophage iron, vascular inflammatory responses, atherosclerotic lesion progression, and plaque stability aforementioned, we further explored the molecular mechanisms by which

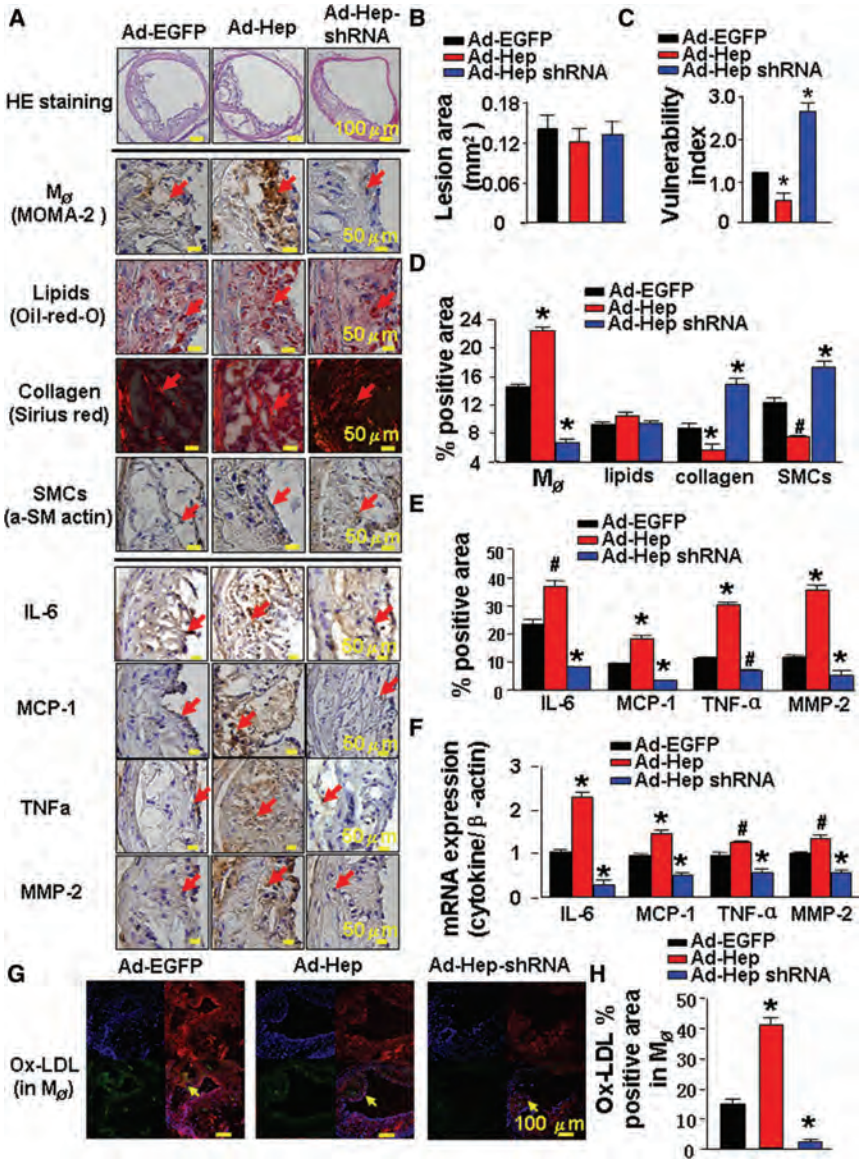

Figure 2. Effects of hepcidin overexpression or knockdown on the plaque composition and inflammatory cytokine expression in 3 groups of mice. **A**, Staining for the carotid plaques, macrophages, lipids, collagen, SMCs, IL-6, MCP-1, TNFα, and MMP-2 in 3 treatment groups. **Arrowheads** indicate positive staining areas. **B**, Lesion area measurements in 3 treatment groups (n=6 in each group). **C**, Vulnerability index in 3 treatment groups (n=6 in each group). **P*<0.01 versus Ad-EGFP group. **D**, Quantitative analysis of the carotid plaque composition in **A** (n=6 in each group). **P*<0.01 versus Ad-EGFP group, #*P*<0.05 versus Ad-EGFP group. **E**, Quantitative analysis of the inflammatory cytokine expression in **A** (n=6 in each group). **P*<0.01 versus Ad-EGFP group, #*P*<0.05 versus Ad-EGFP group. **F**, mRNA expression levels of IL-6, MCP-1, and TNFα in 3 treatment groups. Four polls in each group; 3 arteries as a poll. **P*<0.01 versus Ad-EGFP group, #*P*<0.05 versus Ad-EGFP group. **G**, Intracellular expression of ox-LDL in 3 treatment groups. Blue color indicates macrophage nuclei; red color demonstrates ox-LDL; green color displays macrophages; double staining of red and green depicts ox-LDL expression in macrophages. **Arrowheads** indicate positive staining area. $M_ø$ indicates macrophages. **H**, Quantitative analysis of the results in **G** (n=6 in each group). **P*<0.01 versus Ad-EGFP group.

hepcidin destabilizes plaques in macrophages. Compared with the control, the expression of hepcidin was time- and dose-dependently upregulated in macrophages treated with ox-LDL (Figure 3A). The ox-LDL–induced upregulation of hepcidin was transient, peaked at 2 hours after the stimulation, and thereafter declined to the basal level within 24 hours, with the maximum effective dose of 50 μg/mL (Figure 3A through 3C), suggesting a regulatory role of hepcidin in the ox-LDL–mediated proatherogenic effects such as oxidative stress, inflammatory cytokine secretion, and apoptosis in macrophages. Because hepcidin expression was augmented in intraplaque macrophages (Figure 1D) and the proatherogenic phenotypic switching of macrophages is closely linked with the cellular LDL oxidation and iron loading,[17] the effect of ox-LDL–mediated proatherogenic activation of macrophages was determined in the setting of iron loading by erythrophagocytosis. As postulated, the ox-LDL–induced accumulation of intracellular lipids, upregulation of IL-6, MCP-1, and TNFα expression, augmentations of ROS formation, and apoptosis were further enhanced in the macrophages after erythrophagocytosis (Figure IIA–IIG in the online-only Data Supplement). Interestingly, hepcidin hardly enhanced the ox-LDL–induced proatherogenic activation of macrophages (Figure IIIA–IIIG in the online-only Data Supplement), but the enhancement became quite obvious in the setting of erythrophagocytosis (Figure 3D through 3J), indicating a unique role of hepcidin in ox-LDL–mediated phenotypic modulation of the iron-loaded macrophages. To further study the role of hepcidin in the proatherogenic activation of macrophages after erythrophagocytosis, we applied hepcidin RNA interference approach by using hepcidin siRNA in macrophages. The hepcidin knockdown efficacy was between 70–80% (Materials and Methods in the online-only Data Supplement). The silencing of hepcidin decreased the ox-LDL–induced intracellular lipids accumulation (Figure 4A) and inhibited both basal and ox-LDL–induced inflammatory cytokine expression, oxidative stress, and apoptosis in erythrophagocytosed macrophages (Figure 4B through 4G). Taken together, these results demonstrate that hepcidin is a novel positive regulator of ox-LDL–mediated proatherogenic activation of

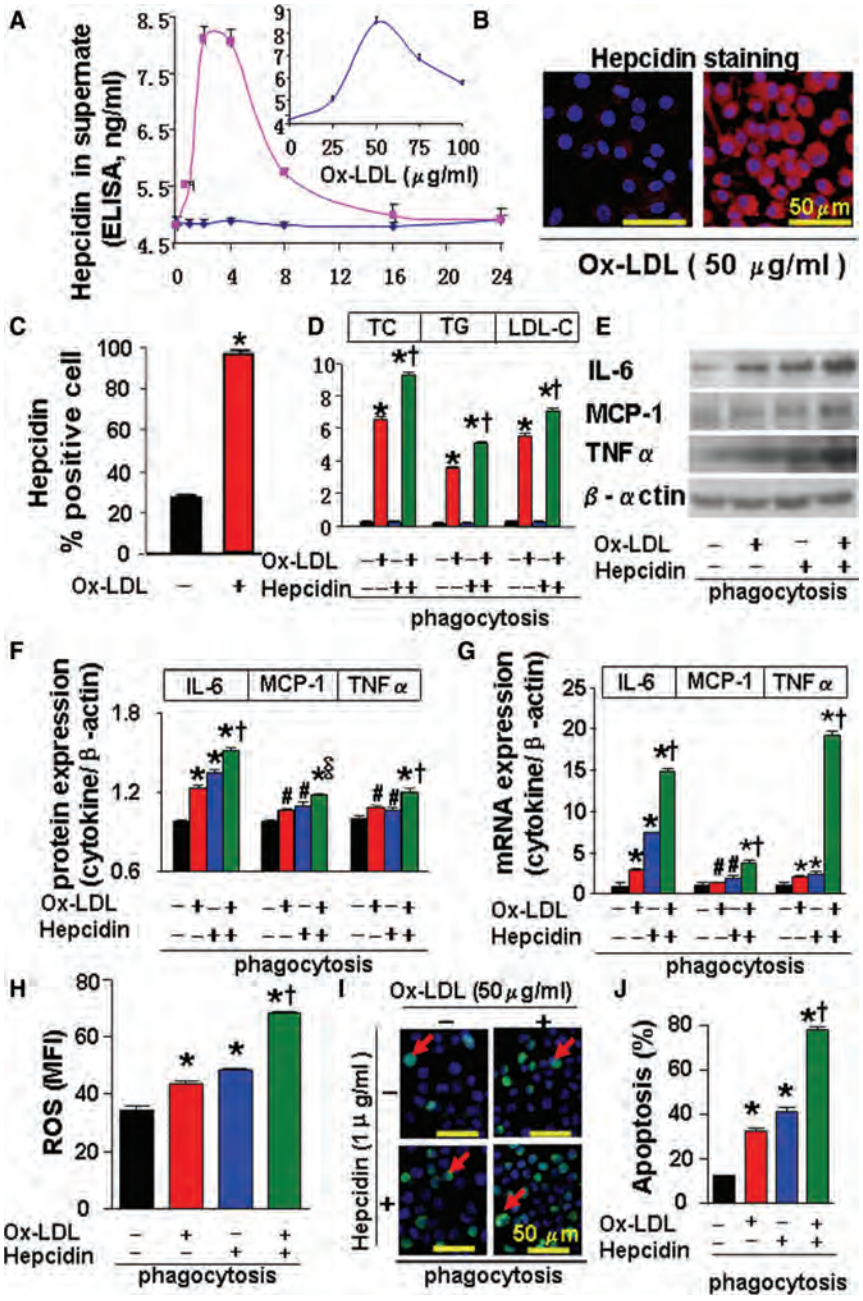

Figure 3. Effects of hepcidin on ox-LDL–induced activation of erythrophagocytosed macrophages in vitro. **A**, Time course of serum hepcidin levels by ELISA after stimulation with or without ox-LDL (50 μg/mL). **Inserted figure** shows serum hepcidin levels in macrophages treated with various concentrations of ox-LDL for 2 hours. **B**, Immunochemical staining for ox-LDL–induced hepcidin expression in macrophages treated with or without ox-LDL (50 μg/mL) for 2 hours. Areas in red indicate hepcidin and areas in blue show nuclei. **C**, Quantitative analysis of hepcidin staining in **B**. **P*<0.01 versus the group without ox-LDL treatment. **D**, Effect of hepcidin on ox-LDL–induced lipid accumulation in erythrophagocytosed macrophages, **P*<0.01 versus control [ox-LDL (−) and hepcidin (−)], †*P*<0.01 versus ox-LDL treatment alone. **E**, Effect of hepcidin on ox-LDL–induced protein expression of IL-6, MCP-1, and TNFα in erythrophagocytosed macrophages. **F**, Quantitative analysis of the results in **E**. **P*<0.01 versus control [ox-LDL (−) and hepcidin (−)], #*P*<0.05 versus control [ox-LDL (−) and hepcidin (−)], †*P*<0.01 versus hepcidin or ox-LDL treatment alone, §*P*<0.05 versus hepcidin or ox-LDL treatment alone. **G**, Effect of hepcidin on ox-LDL–induced mRNA expression of IL-6, MCP-1, and TNFα in erythrophagocytosed macrophages. **P*<0.01 versus control [ox-LDL (−) and hepcidin (−)], #*P*<0.05 versus control [ox-LDL (−) and hepcidin (−)], †*P*<0.01 versus hepcidin or ox-LDL treatment alone. **H**, Effect of hepcidin on ox-LDL–induced ROS formation in erythrophagocytosed macrophages. MFI indicates mean fluorescence intensity. **P*<0.01 versus control [ox-LDL (−) and hepcidin (−)]; †*P*<0.01 versus hepcidin or ox-LDL treatment alone. **I**, Effect of hepcidin on ox-LDL–induced apoptosis in erythrophagocytosed macrophages. Areas in green **(arrowheads)** indicate apoptotic cells and areas in blue depict nuclei. **J**, Quantification of the TUNEL staining in **I**. **P*<0.01 versus control [ox-LDL (−) and hepcidin (−)]; †*P*<0.01 versus hepcidin or ox-LDL treatment alone. All results are representatives of 6 independent experiments.

macrophages in the setting of erythrophagocytosis, contributing to the plaque instability.

Hepcidin-Upregulated Expression of Ferritin in Erythrophagocytosed Macrophages and Atherosclerotic Plaques

Finally, we explored the interplay of iron loading, ox-LDL, and hepcidin in macrophages, which might result in plaque destabilization in vitro and in vivo. We observed a time-dependent upregulation of L-ferritin and H-ferritin, which are iron-storage proteins, and FPN1, an iron-export protein. The expression of FPN1 reached a peak at 4 hours, declined thereafter, and returned to the basal level by 24 hours after erythrophagocytosis, whereas the expression of H-ferritin and L-ferritin reached a peak at 4 hours and 6 hours, respectively, and sustained at least 24 hours after erythrophagocytosis (Figure VA in the online-only Data Supplement). Hepcidin further upregulated the H-ferritin and L-ferritin expression but downregulated the FPN1 expression in the erythrophagocytosed macrophages (Figure 5G and 5H and Figure VB and VC in the online-only Data Supplement). These results demonstrated the critical role of hepcidin in regulating iron levels in the iron-loaded macrophages after erythrophagocytosis as previously described.[18] Importantly, both basal expression and ox-LDL–mediated upregulation of ferritin protein levels were dramatically inhibited by the silencing of hepcidin in erythrophagocytosed macrophages (Figure 5I and 5J). Although there was no significant difference of serum iron levels in the Ad-GFP, Ad-hepcidin, and Ad-hepcidin shRNA groups (Figure 5F), the nonheme iron level and the

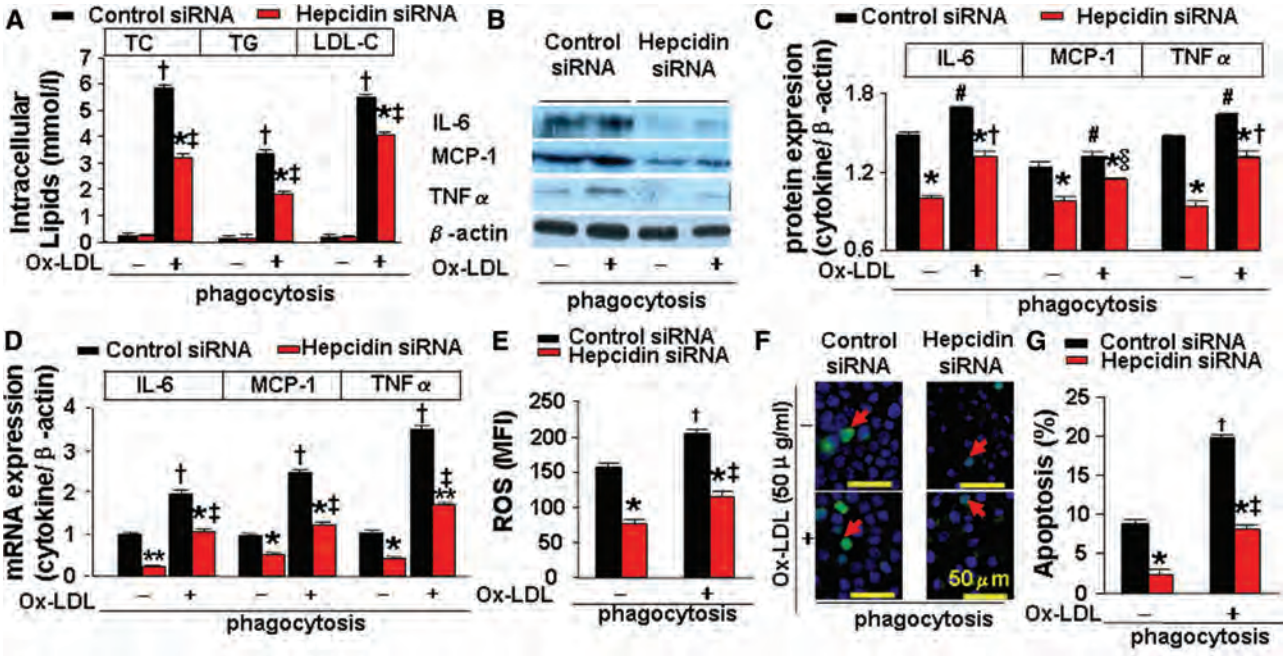

Figure 4. Effects of hepcidin silencing on ox-LDL–induced activation of erythrophagocytosed macrophages in vitro. Macrophages transfected with control siRNA or hepcidin siRNA were subjected to erythrophagocytosis for 2 hours and then treated with or without ox-LDL (50 μg/mL) for 2 hours. **A**, Measurements of intracellular lipids. *$P<0.01$ versus respective control siRNA group treated with or without ox-LDL; †$P<0.01$ versus control siRNA group treated without ox-LDL, ‡$P<0.01$ versus hepcidin siRNA group treated without ox-LDL. **B**, Protein expression levels of IL-6, MCP-1, and TNFα. **C**, Quantitative analysis of the results in **B**. *$P<0.01$ versus respective control siRNA group treated with or without ox-LDL; #$P<0.05$ versus control siRNA group treated without ox-LDL; †$P<0.01$ versus hepcidin siRNA group treated without ox-LDL; §$P<0.05$ versus hepcidin siRNA group treated without ox-LDL. **D**, mRNA expression levels of IL-6, MCP-1, and TNFα. *$P<0.01$ versus respective control siRNA group treated with or without ox-LDL; **$P<0.001$ versus respective control siRNA group treated with or without ox-LDL; †$P<0.01$ versus control siRNA group treated without ox-LDL; ‡$P<0.01$ versus hepcidin siRNA group treated without ox-LDL; **E**, Measurements of ROS formation. MFI indicates mean fluorescence intensity. *$P<0.01$ versus respective control siRNA group treated with or without ox-LDL; †$P<0.01$ versus control siRNA group treated without ox-LDL; ‡$P<0.01$ versus hepcidin siRNA group treated without ox-LDL. **F**, Apoptosis staining by TUNEL. Areas in green (**arrowheads**) indicate apoptotic cells and areas in blue demonstrate nuclei. **G**, Quantitative analysis of the results in **F**. *$P<0.01$ versus respective control siRNA group treated with or without ox-LDL; †$P<0.01$ versus control siRNA group treated without ox-LDL; ‡$P<0.01$ versus hepcidin siRNA group treated without ox-LDL. All results are representative of 6 independent experiments.

expression of Ferritin mRNA and protein in the atherosclerotic plaque was upregulated or downregulated by the local adenoviral overexpression of hepcidin or by its shRNA, respectively (Figure 5A through 5E). These results demonstrate that hepcidin controls iron trapping in erythrophagocytosed macrophages and atherosclerotic lesions.

Considering a key role of hepcidin in elevating ox-LDL levels in intraplaque macrophages (Figure 2G and 2H) and the suppression of hepcidin inhibitor on lipid accumulation, iron retention, and ROS formation,[10] we further determined the potential interaction of hepcidin, iron retention, and ox-LDL loading on proatherosclerotic activation of macrophages. Macrophage intracellular iron was scavenged by iron chelators including DFO and ferrous chelator BPDL as described elsewhere (Figure IVA and IVB in the online-only Data Supplement),[14,15] The increased lipids accumulation, proinflammatory cytokine production, ROS formation, and apoptosis in erythrophagocytosed macrophages were inhibited by adding of DFO and BPDL (Figure IVC–IVI in the online-only Data Supplement), indicating that the trapped iron in erythrophagocytosed macrophages is redox active. Moreover, erythrophagocytosis per se had a minor effect on the intracellular levels of lipids including TC, TG, and LDL-C in the macrophages without ox-LDL loading (Figure IIA in the online-only Data Supplement), and the adding of DFO and BPDL hardly affected the lipid levels in the phagocytosed macrophages without ox-LDL treatment (Figure IVC in the online-only Data Supplement). However, the elevated intracellular lipid levels in macrophages due to ox-LDL loading were further augmented by erythrophagocytosis (Figure IIA in the online-only Data Supplement). These results suggest that trapped iron promotes lipid accumulation in macrophages at a setting of proatherosclerotic dysregulation of lipid metabolism. Whereas the synergistic effect of ox-LDL loading and erythrophagocytosis on intracellular lipid accumulation in macrophages was inhibited by hepcidin silencing (Figure 4A) and the iron chelators (Figure IVC in the online-only Data Supplement), it was further enhanced by hepcidin (Figure 3D). Taken together, these findings support a notion that the interaction of hepcidin, trapped iron, and accumulated lipids is critical for proatherosclerotic activation of macrophages contributing to destabilization.

Discussion

In this study, we provided several novel findings regarding the hepcidin-mediated atherosclerosis as follows: (1) Hepcidin is a positive regulator of atherosclerotic plaque instability; (2) hepcidin is essential for ox-LDL–mediated phenotypic switching of iron-loaded macrophages leading to atherosclerotic plaque destabilization; (3) hepcidin upregulates

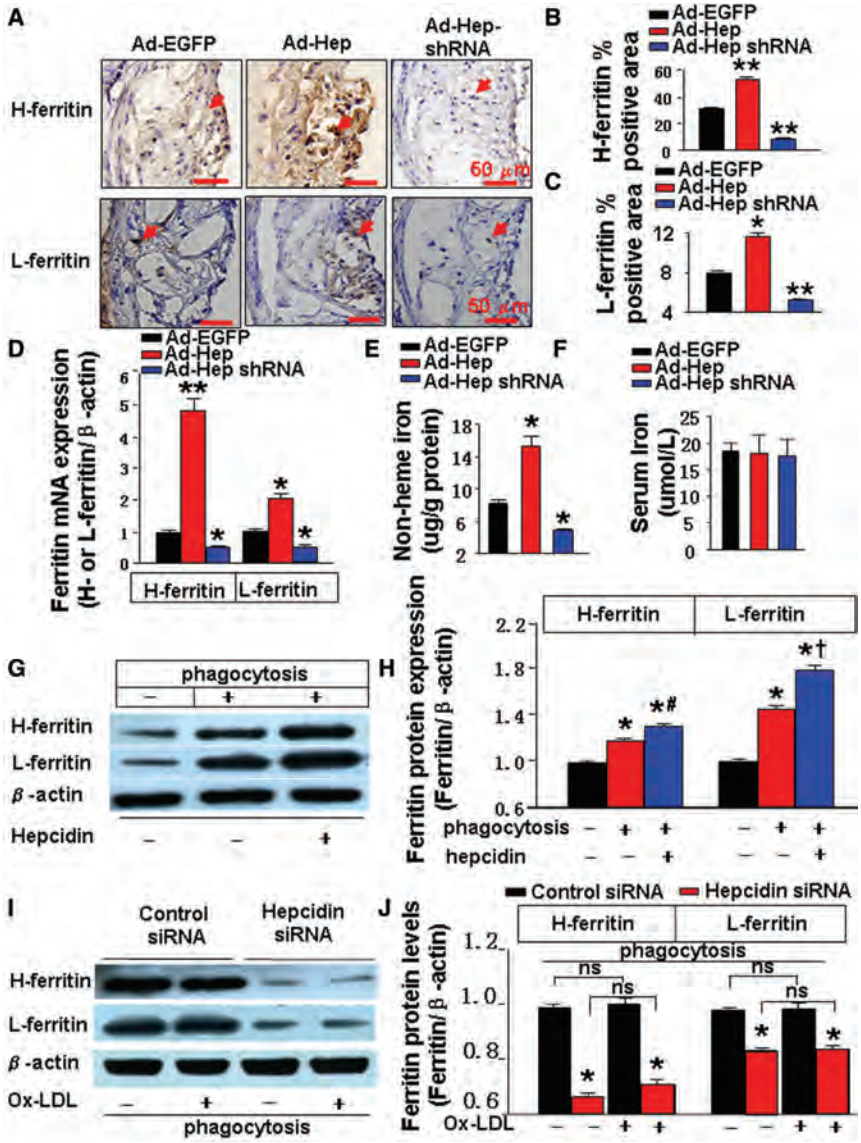

Figure 5. Effects of hepcidin on ferritin expression in erythrophagocytosed macrophages in vitro and atherosclerotic plaques in vivo. **A**, Immunochemical staining for H-ferritin and L-ferritin **(arrowheads)** in carotid plaques in 3 treatment groups. **B**, Quantification of H-ferritin expression in **A**. $^{**}P<0.001$ versus Ad-EGFP group (n=6 in each group). **C**, Quantification of the L-ferritin expression in **A**. $^{*}P<0.01$ versus Ad-EGFP group; $^{**}P<0.001$ versus Ad-EGFP group. **D**, mRNA expression of H-ferritin and L-ferritin in 3 treatment groups. $^{*}P<0.01$ versus Ad-EGFP group; $^{**}P<0.001$ versus Ad-EGFP group. **E**, Non-heme iron levels in the carotid plaques of 3 treatment groups. $^{*}P<0.01$ versus Ad-EGFP group (n=4 in each group). **F**, Serum iron levels of 3 treatment groups (n=6 in each group). **G**, H-ferritin and L-ferritin protein expression in erythrophagocytosed macrophages treated with or without hepcidin (1 μg/mL) for 2 hours. **H**, Quantitative analysis of the results in **G**. $^{*}P<0.01$ versus macrophages without erythrophagocytosis; †$P<0.01$ versus erythrophagocytosed macrophages without hepcidin treatment; #$P<0.05$ versus erythrophagocytosed macrophages without hepcidin treatment. (n=6). **I**, Macrophages transfected with control siRNA or hepcidin siRNA were subjected to erythrophagocytosis for 2 hours and then treated with or without ox-LDL (50 μg/mL) for 2 hours. H-ferritin and L-ferritin protein expression was measured by Western blot. **J**, Quantitative analysis of the results in **I**. $^{*}P<0.01$ versus respective control siRNA group treated with or without ox-LDL (n=6).

ferritin trapping iron in macrophages, whereas iron loading in turn facilitates the hepcidin-mediated phenotypic switch of macrophages; and (4) the interaction of hepcidin, trapped iron, and accumulated lipids is critical for proatherosclerotic activation of macrophages contributing to destabilization. To our knowledge, these results demonstrate for the first time that hepcidin is a positive regulator of atherosclerotic plaque destabilization via regulating iron homeostasis in macrophages.

Although iron retention as a key mechanism of atherosclerosis has been proposed for decades,[19] only recently did some authors find that the storage and processing of iron from erythrophagocytosis by macrophages within plaque is an important source of iron retention in atherosclerotic lesions.[20] Loading of iron in macrophages promotes lipid accumulation and induces oxidative stress.[17] Oxidative reactions associated with the overloaded iron and lipids facilitate macrophage apoptosis with the release of cellular contents into the lesion, which further enhances inflammatory responses. In contrast, administration of desferrioxamine, an iron chelator, attenuated inflammation and macrophage-specific gene expression in atherosclerotic lesions of ApoE$^{-/-}$ mice.[14] A recent study found that pathological iron metabolism in macrophages contributes to vulnerability of human carotid plaque.[21] However, the critical regulator of the phenotypic switching of the iron loaded macrophages remains to be verified. In this context, our results demonstrated that there is the endogenous expression in the atherosclerotic plaque and hepcidin is a critical mediator of plaque destabilization and ox-LDL–exaggerated lipids accumulation, oxidative stress, inflammation, and apoptosis in macrophages after erythrophagocytosis, thus providing a novel insight into the understanding of "iron hypothesis" in the pathogenesis of atherosclerosis.[19] In addition, we observed that hepcidin downregulated FPN1 expression and upregulated L-ferritin and H-ferritin expression in macrophages after erythrophagocytes. Since hepcidin has been demonstrated to suppress iron release from macrophages after erythrophagocytosis via downregulating the expression of iron-export FPN1,[6] and ferritin is an iron-storage protein,[22] it is most likely that hepcidin suppresses

iron release from proatherogenically activated macrophages via both inhibiting iron export and increasing iron storage. With the consideration of the fact that hepcidin did not facilitate ox-LDL–induced proatherogenic activation of macrophages until an onset of erythrophagocytosis, it is conceivable that loading iron and upregulating hepcidin might form a positive feedback loop in the phenotypic modulation of macrophages leading to the plaque instability. This notion is actually supported by a recent study demonstrating that hepcidin and macrophage iron correlate with vascular damage in high-risk individuals with metabolic alterations.[9] The "iron hypothesis" that iron deficiency may play a protective role against atherosclerosis has been criticized by the lack of an increased risk for arterial structural lesions in genetic hemochromatosis.[23] However, the very low level of hepcidin concentration with decreased retention of iron in macrophages in hemochromatosis may explain this paradox, though the precise mechanism remains to be explored.[24] This study not only revealed a unique role of hepcidin in mediating plaque instability but also provided direct evidence to clarify the paradoxical issues observed in hemochromatosis.

As observed, the expression of IL-6, MCP-1, TNFα, and MMP-2 was enhanced by hepcidin in atherosclerotic lesions; meanwhile, several studies revealed that hepcidin could be induced by inflammation cytokines.[25] Therefore, at certain stages of plaque progression, inflamed atherosclerotic tissue may upregulate the production of hepcidin, which in turn augments macrophage iron retention and iron-associated inflammation. Moreover, we observed that trapped iron was not able to augment intracellular lipid accumulation in macrophages until an ox-LDL loading, and hepcidin increased intracellular lipid level only in macrophages with trapped iron as well as ox-LDL loading. Collectively, these findings indicate that the interaction of hepcidin, trapped iron, and accumulated lipids is critical for proatherosclerotic activation of macrophages leading to plaque destabilization. Our results were consistent with a recent report that pharmacological suppression of hepcidin decreased lipid accumulation, intracellular iron, and ROS formation in macrophages.[10] However, in contrast to their finding that systemic suppression of hepcidin inhibited early aortic lesion formation, our study found that local knockdown of hepcidin did not affect the size of advanced carotid plaques in mice. It is likely that short-term manipulation of hepcidin expression in an already established plaque may not be adequate to assess the role of hepcidin in plaque formation, and further studies are warranted to address this important issue.

It has been recently documented that intraplaque hemorrhage not only stimulates the progression of atherosclerosis but also promotes the transition of plaques from a stable to an unstable lesion.[26] Moreover, plaques with this intraplaque hemorrhage are vulnerable to new plaque hemorrhage.[27] In a rabbit model of intraplaque hemorrhage, we found that erythrocytes may induce plaque destabilization in a dose-dependent fashion.[3] Many substances including iron were released from hemoglobin and taken by macrophages via CD163 receptor.[28] Meanwhile, the expression of hepcidin is promoted by inflammation, which leads to the more iron retention in macrophages. Thus, whether hepcidin regulates CD163 receptor function to participate in the intraplaque hemorrhage-induced atherosclerosis progression deserves further investigation.

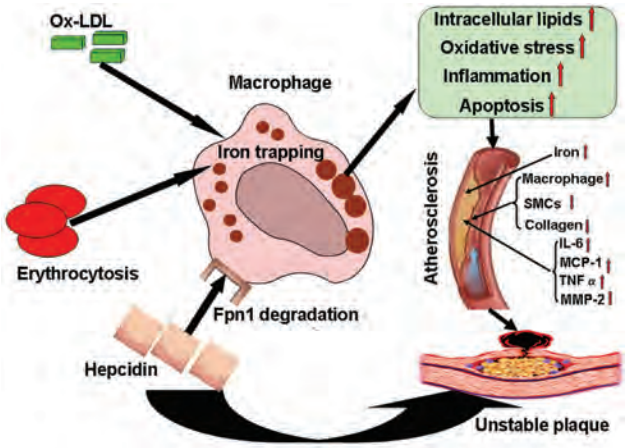

Figure 6. Proposed mechanisms underlying hepcidin-induced plaque instability. In the setting of erythrophagocytosis, hepcidin suppresses iron release from macrophages via downregulating the expression of iron-export FPN1 and increases iron storage. Iron trapping results in accumulated intracellular lipids and enhanced oxidative stress, inflammatory responses, and macrophage apoptosis. Thus, hepcidin is essential for ox-LDL–mediated phenotypic switching of iron-loaded macrophages leading to atherosclerotic plaque destabilization.

In summary, we showed that in a mouse model of atherosclerosis, the expression of hepcidin was upregulated in atherosclerotic plaque and that hepcidin is a positive regulator of plaque instability and inflammation. Only in the setting of erythrophagocytosis did hepcidin preferentially enhance the ox-LDL–induced proatherogenic activation of macrophages leading to plaque destabilization. Hepcidin upregulated the expression of ferritin in erythrophagocytosed macrophages and atherosclerotic plaques, and the iron trapping might be critical for the hepcidin-mediated phenotypic switching of macrophages leading to the plaque instability (Figure 6).

Acknowledgments

We thank Prof Guo Qing Liu at Beijing University, Prof Zhong Ming Qian at Hongkong Polytechnic University, and Prof Ming Xiang Zhang, Prof Fan Jiang, Prof Fan Yi, Dr Chun Xi Liu, Dr Xu Ping Wang, and Dr Hong Jiang at Shandong University for their excellent technical assistance.

Sources of Funding

This work was supported by the National 973 Basic Research Program of China (No. 2012CB518603, 2011CB503906), the National High-tech Research and Development Program of China (No. 2012AA02A510), the Program of Introducing Talents of Discipline to Universities (No. B07035), the State Program of National Natural Science Foundation of China for Innovative Research Group (No. 81021001), the State Key Program of National Natural Science of China (No. 60831003), grants of the National Natural Science Foundation of China (No. 30900607, 30971096, 30972809, 81100206, 81173251, 81170207, 81000126), grants of the Natural Science Foundation of Shandong Province, P. R. China (No. ZR2011HQ039), and the Foundation for Excellent Young Scientists of Shandong Province, P. R. China (No. BS2009SW026).

Disclosures

None.

References

1. Ishizaka N, Saito K, Furuta K, Matsuzaki G, Koike K, Noiri E, Nagai R. Angiotensin II-induced regulation of the expression and localization of iron metabolism-related genes in the rat kidney. *Hypertens Res*. 2007;30:195–202.
2. Sullivan JL. Iron and the genetics of cardiovascular disease. *Circulation*. 1999;100:1260–1263.
3. Lin HL, Xu XS, Lu HX, Zhang L, Li CJ, Tang MX, Sun HW, Liu Y, Zhang Y. Pathological mechanisms and dose dependency of erythrocyte-induced vulnerability of atherosclerotic plaques. *J Mol Cell Cardiol*. 2007;43:272–280.
4. Theurl I, Mattle V, Seifert M, Mariani M, Marth C, Weiss G. Dysregulated monocyte iron homeostasis and erythropoietin formation in patients with anemia of chronic disease. *Blood*. 2006;107:4142–4148.
5. Nguyen NB, Callaghan KD, Ghio AJ, Haile DJ, Yang F. Hepcidin expression and iron transport in alveolar macrophages. *Am J Physiol Lung Cell Mol Physiol*. 2006;291:L417–L425.
6. Nemeth E, Tuttle MS, Powelson J, Vaughn MB, Donovan A, Ward DM, Ganz T, Kaplan J. Hepcidin regulates cellular iron efflux by binding to Ferroportin and inducing its internalization. *Science*. 2004;306:2090–2093.
7. Theurl I, Theurl M, Seifert M, Mair S, Nairz M, Rumpold H, Zoller H, Bellmann-Weiler R, Niederegger H, Talasz H, Weiss G. Autocrine formation of hepcidin induces iron retention in human monocytes. *Blood*. 2008;111:2392–2399.
8. Sullivan JL. Macrophage iron, hepcidin, and atherosclerotic plaque stability. *Exp Biol Med (Maywood)*. 2007;232:1014–1020.
9. Valenti L, Dongiovanni P, Motta BM, Swinkels DW, Bonara P, Rametta R, Burdick L, Frugoni C, Fracanzani AL, Fargion S. Serum hepcidin and macrophage iron correlate with MCP-1 release and vascular damage in patients with metabolic syndrome alterations. *Arterioscler Thromb Vasc Biol*. 2011;31:683–690.
10. Saeed O, Otsuka F, Polavarapu R, Karmali V, Weiss D, Davis T, Rostad B, Pachura K, Adams L, Elliott J, Taylor WR, Narula J, Kolodgie F, Virmani R, Hong CC, Finn AV. Pharmacological suppression of hepcidin increases macrophage cholesterol efflux and reduces foam cell formation and atherosclerosis. *Arterioscler Thromb Vasc Biol*. November 17, 2011 [Epub ahead of print].
11. von der Thusen JH, van Berkel TJ, Biessen EA. Induction of rapid atherogenesis by perivascular carotid collar placement in apolipoprotein E-deficient and low-density lipoprotein receptor-deficient mice. *Circulation*. 2001;103:1164–1170.
12. Shiomi M, Ito T, Hirouchi Y, Enomoto M. Fibromuscular cap composition is important for the stability of established atherosclerotic plaques in mature WHHL rabbits treated with statins. *Atherosclerosis*. 2001;157:75–84.
13. Knutson MD, Vafa MR, Haile DJ, Wessling-Resnick M. Iron loading and erythrophagocytosis increase Ferroportin 1 (FPN1) expression in J774 macrophages. *Blood*. 2003;102:4191–4197.
14. Zhang WJ, Wei H, Frei B. The iron chelator, desferrioxamine, reduces inflammation and atherosclerotic lesion development in experimental mice. *Exp Biol Med (Maywood)*. 2010;235:633–641.
15. Breuer W, Epsztejn S, Cabantchik ZI. Iron acquired from transferrin by K562 cells is delivered into a cytoplasmic pool of chelatable iron(II). *J Biol Chem*. 1995;270:24209–24215.
16. Ross R. Atherosclerosis: an inflammatory disease. *N Engl J Med*. 1999;340:115–126.
17. Kraml PJ, Klein RL, Huang Y, Nareika A, Lopes-Virella MF. Iron loading increases cholesterol accumulation and macrophage scavenger receptor I expression in THP-1 mononuclear phagocytes. *Metabolism*. 2005;54:453–459.
18. Delaby C, Pilard N, Goncalves AS, Beaumont C, Canonne-Hergaux F. Presence of the iron exporter Ferroportin at the plasma membrane of macrophages is enhanced by iron loading and downregulated by hepcidin. *Blood*. 2005;106:3979–3984.
19. Sullivan JL. Iron and the sex difference in heart disease risk. *Lancet*. 1981;1:1293–1294.
20. Yuan XM, Anders WL, Olsson AG, Brunk UT. Iron in human atheroma and LDL oxidation by macrophages following erythrophagocytosis. *Atherosclerosis*. 1996;124:61–73.
21. Li W, Xu LH, Forssell C, Sullivan JL, Yuan XM. Overexpression of transferrin receptor and ferritin related to clinical symptoms and destabilization of human carotid plaques. *Exp Biol Med (Maywood)*. 2008;233:818–826.
22. Ponka P. Cellular iron metabolism. *Kidney Int Suppl*. 1999;69:S2–S11.
23. Franco RF, Zago MA, Trip MD, ten Cate H, van den Ende A, Prins MH, Kastelein JJ, Reitsma PH. Prevalence of hereditary haemochromatosis in premature atherosclerotic vascular disease. *Br J Haematol*. 1998;102:1172–1175.
24. Sullivan JL. Do hemochromatosis mutations protect against iron-mediated atherogenesis? *Circ Cardiovasc Genet*. 2009;2:652–657.
25. Lee P, Peng H, Gelbart T, Beutler E. The IL-6- and lipopolysaccharide-induced transcription of hepcidin in HFE-, transferrin receptor 2-, and beta 2-microglobulin-deficient hepatocytes. *Proc Natl Acad Sci U|S|A*. 2004;101:9263–9265.
26. Kolodgie FD, Gold HK, Burke AP, Fowler DR, Kruth HS, Weber DK, Farb A, Guerrero LJ, Hayase M, Kutys R, Narula J, Finn AV, Virmani R. Intraplaque hemorrhage and progression of coronary atheroma. *N Engl J Med*. 2003;349:2316–2325.
27. Rao DS, Goldin JG, Fishbein MC. Determinants of plaque instability in atherosclerotic vascular disease. *Cardiovasc Pathol*. 2005;14:285–293.
28. Kovtunovych G, Eckhaus MA, Ghosh MC, Ollivierre-Wilson H, Rouault TA. Dysfunction of the heme recycling system in heme oxygenase 1-deficient mice: effects on macrophage viability and tissue iron distribution. *Blood*. 2010;116:6054–6062.

Supplement Material

Hepcidin Destabilizes Atherosclerotic Plaque via Over-activating Macrophages after Erythrophagocytosis

Jing Jing Li[1*], Xiao Meng[1*], Hai Peng Si[2], Cheng Zhang[1], Hui Xia Lv[1], Yu Xia Zhao[1], Jian Min Yang[1], Mei Dong[1], Kai Zhang[1], Su Xia Liu[1], Xue Qiang Zhao[1], Fei Gao[1], Xiao Ling Liu[1], Taixing Cui[3†], Yun Zhang[1†]

First Author Surname: Li and Meng

Running Title: Hepcidin Destabilizes Atherosclerotic Plaque

[1]The Key Laboratory of Cardiovascular Remodeling and Function Research, Chinese Ministry of Education and Chinese Ministry of Health, Shandong University, Jinan, Shandong, 250012, China; [2]Department of Orthopedics, Second Hospital, Shandong University, Jinan, Shandong, 250012, China; [3]Department of Cell Biology and Anatomy, University of South Carolina School of Medicine, Columbia, SC, 29208, USA.

*These authors equally contribute to this work.

Correspondence to Yun Zhang, M.D., Ph.D., F.A.C.C., E-mail: zhangyun@sdu.edu.cn , or Taixing Cui, M.D., Ph.D., E-mail:

Taixing.Cui@uscmed.sc.edu, Qilu Hospital, Shandong University No.107, Wen Hua Xi Road, Jinan, Shandong, 250012, P.R. China, Tel: +86-531-82169139; Fax: +86-531-86169358

Materials and Methods

Preparation of Adenoviral Vectors

The murine hepcidin cDNA （NM_032541.1) was amplified by Reverse transcription polymerase chain reaction (RT-PCR), cloned into pMD18-T vector (Invitrogen, USA), and then sub-cloned into pIRES2-EGFP vector using the EcoRI and BamH I sites. The hepcidin cDNA sequence was confirmed by sequencing. A shRNA sequence (5'-uucagaugagacagacuacagaa-3' and 5'-uucuguagucugucucaucugaa-3') that is used to target hepcidin was cloned into the pcDNA™6.2-GW/EmGFPmiR vector (Invitrogen, USA) and confirmed by sequencing. Both hepcidin and its shRNA IRES2-EGFP cassettes were cloned into the adenoviral expression vector pAd/CMV/V5/DEST using the Gateway Technology (Invitrogen, USA). Recombinant viruses were packaged and amplified in HEK293 cells (Department of Cells, Chinese Academy of Sciences, Shanghai, China) and purified by anion chromatography. The titer of the viral vectors was determined by TCID50 (Tissue culture infective dose) method. The adenoviral vectors expressing EGFP alone (Ad-EGFP) were used as control.

Animal Model and Gene Transfer

Our study in animal models consisted of two parts. In the first part of the *in vivo* study, forty male apoE−/− mice (6 weeks of age; Beijing University, Beijing, China) were randomly divided into a control group (n=20) and a model group (n=20), and were housed at a constant temperature (24 ˚C) in a room under 12-h dark/12-h light cycles. Mice in the control group were given a normal diet for 13 weeks and then euthanized. Mice in the model group were received a high-fat diet (0.25% cholesterol and 15% cocoa butter) for 2 weeks and then a constrictive silastic tube (0.30-mm inner diameter,

0.50-mm outer diameter, and 2.5-mm long; Shandong Key Laboratory of Medical Polymer Materials, Jinan, China) was placed around the left common carotid artery near its bifurcation as previously described.[1] These mice were maintained on a high-fat diet for additional 11 weeks. The left common carotid arteries in both groups of mice were collected for histological and molecular biological analysis.

In the second part of the *in vivo* study, seventy-five male apoE−/− mice (6 weeks of age; Beijing University, Beijing, China) were given a high-fat diet (0.25% cholesterol and 15% cocoa butter) for 2 weeks. Then a constrictive silastic tube (0.30-mm inner diameter, 0.50-mm outer diameter, and 2.5-mm long; Shandong Key Laboratory of Medical Polymer Materials, Jinan, China) was placed around the left common carotid artery near its bifurcation. Eight weeks after the collar placement, mice were randomly divided into three groups (n=25 each) for adenoviral gene delivery of EGFP, EGFP-hepcidin, and EGFP-hepcidin shRNA at a dose of 3.12×10^9 ifu, respectively. Local adenoviral infection was induced as previously described.[2] Briefly, mice were anesthetized with an intraperitoneal injection of pentobarbital sodium (40 mg/kg), the collars were removed, and adenoviral suspension was instilled into the left common carotid artery via the left external carotid artery for 15 minutes, and then drawn off before ligation of the external carotid artery and closure of the skin wound with silk sutures. These mice were maintained on a high-fat diet for additional 3 weeks, and then euthanized. The left common carotid arteries in the three groups of mice were collected for pathological and molecular biological analysis. Two mice in each of the three groups were euthanized at one week and two weeks after the infection to determine the

efficiency of the adenoviral gene delivery in atherosclerotic plaque. Cryosections were viewed on fluorescence microscopy to identify GFP expression.

All animal care and procedures were approved by Shandong University Institutional Animal Care and Use Committee and complied with the *Guide for the Use and Care of Laboratory Animals* published by the US National Institutes of Health (NIH publication 80-23, revised 1996)

Serum Lipid, Glucose and Iron Measurement

At the end of the second part of the *in vivo* study, blood was collected from the inferior vena cava before perfusion-fixation. Serum total cholesterol (TC), triglycerides (TG), low-density lipoprotein cholesterol (LDL-C), and high-density lipoprotein cholesterol (HDL-C) and glucose concentrations were measured by enzymatic assay. Serum iron levels were measured with Iron (FE) Reagent by Synchron LX Systems (Beckman Coulter, Inc, Fullerton, USA).

Tissue Preparation and Histological Analysis

After euthanasia, mice were perfused with PBS through the left ventricle and then underwent perfusion fixation at 100mm Hg with 4% formaldehyde (pH 7.2) for 15 minutes. The left common carotid artery with bifurcation was carefully excised and immersed in 4% formaldehyde overnight (4°C), embedded in optical coherence tomography compound, and stored at –20°C until use. Each vessel throughout the entire length of the carotid artery underwent histological analysis.

Serial sections were cut at 6 μm thickness every 50 μm along the carotid artery specimens. The site of maximal plaque size was selected for morphologic analysis. Sections were stained with hematoxylin and eosin. Collagen was visualized by sirius red

staining. Lipid deposition was identified by Oil-red O staining. Corresponding sections on separate slides were immunostained with the following antibodies: anti-monocyte/macrophage monoclonal antibody (MOMA-2, 1:150, Serotec, Oxford, UK), anti-α-smooth muscle (SM) actin monoclonal antibody (1:100, Sigma, St. Louis, MO, USA), anti-interleukin-6 (IL-6) polyclonal antibody (1:200, Abcam, Cambridge,UK), anti-tumor necrosis factor-α (TNF-α) monoclonal antibody (1:100, Abcam, Cambridge, UK), anti-monocyte chemoattractant protein-1 (MCP-1) antibody (1:100, R&D Systems, Minneapolis , USA), anti-matrix metalloproteinase (MMP-2) monoclonal antibody (1:100, Abcam, Cambridge, UK), anti-hepcidin monoclonal antibody (1:150, Abcam, Cambridge, UK), anti-L-ferritin antibody (1:100, Abcam, Cambridge, UK) and anti-H-ferritin antibody (1:100, Santa Cruz Biotechology, INC). After incubation with the appropriate horseradish peroxidase (HRP)-conjugated secondary antibodies, the sections were incubated with 3',3'-diaminobenzidine and counterstained with hematoxylin. Sections reacted with non-immune IgG and secondary antibodies were used as negative controls.

Positive staining areas of macrophages, smooth muscle cells (SMCs), lipids, collagen, IL-6, MCP-1, TNF-α, MMP-2, hepcidin, H-ferritin and L-ferritin were quantified by computer-assisted color-gated measurement, and the ratios of the positive staining area to the arterial cross sectional area (part 1 *in vivo* study) or plaque area (part 2 *in vivo* study) were calculated by an automated image analysis system (Image-Pro Plus 6.0, Media Cybernetics, USA). The vulnerable index was calculated by the following formula: the relative positive staining area of (macrophages% +lipid%) / the relative positive staining area of (α-SMCs% +collagen%).[2]

Immunofluorescence

Tissue sections of the left common carotid arteries were incubated with the double primary antibodies, including those against macrophages (MOMA-2, AbD Serotec, UK) and hepcidin (Abcam, UK), α-smooth muscle actin (SMC, Abcam, UK) and hepcidin, macrophages and ox-LDL (1:100, Abcam, UK), as well as α-smooth muscle actin and ox-LDL at 4℃ overnight. Alexa Fluor 555 and 633 labeled IgG were used as secondary antibody. 4', 6-diamidino-2-phenylindole (DAPI) was applied to display the cell nuclei and fluorescent images were obtained by a laser scanning confocal microscopy (LSM710, Carl Zeiss, Germany). The ratio of the positive double staining area of macrophages and ox-LDL to the positive staining area of macrophages were calculated by an automated image analysis system (Image-Pro Plus 6.0, Media Cybernetics, USA).

Cell Culture and Treatment

Macrophage culture

J774 macrophages were chosen for erythrophagocytosis as previously described [3, 4], which were purchased from ATCC and cultured in DMEM medium (GIBCO, Grand Island, NY) containing 10% fetal bovine serum, 100 U/mL penicillin, and 100 g/mL streptomycin at 37°C in 5% CO_2.

Erythrophagocytosis

Erythrophagocytosis was performed as previously described with slight modifications.[3] Briefly, the isolated mouse erythrocytes (2×10^9) were opsonized with goat anti-mouse IgG (1:20; Rockland, Gilbertsville , USA) at 37°C for 20 minutes and then were washed twice in 20 volumes of Alsever's solution (Sigma, St. Louis, MO, USA). The opsonized erythrocytes (2×10^7) were added to J774 macrophage monolayers (2×10^6) and incubated for 2 hours at 37°C with a final ratio of red blood cells to J774 cells at about

9:1. After uptake, noningested opsonized erythrocytes were removed using Red Blood Cell Lysis Buffer (Beyotime Institute, Shanghai, China) followed by 3 washes with PBS. Control cells were subjected to the same lysis and washing steps as cells treated with erythrocytes. Cell viability at the end of the treatment was confirmed by the fact that more than 99% of the J774 macrophages excluded trypan blue, indicating erythrophagocytosis *per se* did not cause cell death.

To examine the effect of ox-LDL on hepcidin expression, ox-LDL (0-100μg/ml, Peking Union Medical College, Beijing, China) was added to the J774 macrophage monolayers (2×10^6) and the cells were incubated for 1, 2, 4, 8, 16 and 24 hours.

Monolayers of J774 macrophages (2×10^6) or J774 macrophages after erythrophagocytosis (2×10^6) were treated with ox-LDL (50μg/ml), synthetic human hepcidin (1μg/ml, Abcam, Cambridge, UK) and/or ferric iron chelator desferrioxamine (DFO, 200 μM, Novartis Pharma, Basel, Switzerland) and ferrous chelator 2,2'-bipyridyl (BPDL, 100 μM, Sigma, St. Louis, MO, USA) as indicated for 2 hours.

Hepcidin silence in cultured macrophages was achieved by hepcidin RNA interference approach. Specific siRNA targeting mouse hepcidin, control siRNA, and Lipofectamine TM 2000 were purchased from Invitrogen (Carlsbad, USA). Positive duplexes (hepcidin-siRNA) were 5'-uucagaugagacagacuacagaa-3' and 5'-uucuguagucugucucaucugaa-3', negative duplexes (Control siRNA) were 5'-uucuccgaacgugucacgutt-3' and 5'-acgugacacguucggagaatt-3'.

J774 macrophages were seeded at 50% confluence in DMEM supplemented with 10% FBS without antibiotics. Twenty-four hours after plating, cells were transfected with 150 nM hepcidin siRNA or control siRNA using Lipofectamine TM 2000, and cells were

harvested 36 hours later. The hepcidin knockdown efficacy was between 70% and 80% as confirmed by hepcidin mRNA levels measured by quantitative real-time PCR.

Monolayers of J774 macrophages transfected with control or hepcidin siRNAs (2×10^6) were subjected to erythrophgaocytosis for 2 hours, and then treated with or without ox-LDL (50 μg/ml), DFO (200 μM) and BPDL (200 μM) in serum-free medium for 2 hours.

Quantitative Real-time-PCR

The left common carotid arteries and the J774 macrophage with different treatments were extracted with TriZol Reagent (Invitrogen, Carlsbad, USA) according to the manufacturer's instruction. Primers were designed using Beacon Designer 2.0 software (Bio-Rad, Hercules, CA), and were chemically synthesized by Integrated DNA Technologies (Coralville, IA). The primers used in this study were as follows: hepcidin: sense, 5'-CGATACCAATGCAGAAGAGAAGG-3', and antisense, 5'-TTCAAGGTCATTGGTGGGGA-3'; IL-6: sense, 5'-AGTCACAGAAGGAGTGGCTAAG-3', and antisense, 5'-GAGGAATGTCCACAAACTGATA-3'; MCP-1: sense, 5'-AGCCAGATGCAGTTAACGC-3', and antisense, 5'-GCCTACTCATTGGGATCATCTTG-3'; TNF-α: sense, 5'-TGTTCATCCATTCTCTACCC-3', and antisense 5'-TCACTGTCCCAGCATCTTGT-3'; MMP-2: sense 5'-TTCAAGGACCGGTTCATTTGGCGGACTGTG-3', and antisense 5'-TTCCAAACTTCACGCTCTTCAGACTTTGGTT-3', Ferroportin1 (FPN1): sense , 5'-CCAAGGCAAGAGATCAAACCC-3', and antisense 5'-CCACCAGAAACACAGACACTGC-3'; L-ferritin: sense, 5'-GATCAACCTGGAGTTGTATGCC-3', and antisense 5'-CTCCCAGTCATCACGGTCTG-

3', H-ferritin: sense, 5'-CCATCAACCGCCAGATCAAC-3', and antisense 5'-GCCACATCATCTCGGTCAAA-3', β-actin: sense, 5'-CACTGTGCCCATCTACGA-3', and antisense, 5'-GTAGTCTGTCAGGTCCCG-3'.

The extracted RNA was dissolved in a final volume of 25 μL RNase-free water, and the concentrations were determined by spectrophotometry. One microgram of mRNA was reversely transcribed using iScript cDNA synthesis kit (Bio-Rad, Hercules, CA) in a final volume of 20 μL. One microliter of cDNA in a 25-μL volume was used for real-time PCR with an SYBR Green I Supermix kit (Bio-Rad). PCR was performed in duplicate using the Light Cycler (Roche, Basel, Switzerland) real-time PCR detection system for 40 cycles at 95°C for 10 sec, 58°C for 20 sec, and 72°C for 30 sec. The data were analyzed by Light Cycler software 4.0 (Roche). Hepcidin, Il-6, MCP-1, TNF-α, MMP-2, FPN1, L-ferritin and H-ferritin expression was normalized to that of β-actin.

Western Blot Analysis

The total protein of J774 macrophages with different treatments were extracted respectively, and protein concentrations were measured using a Bio-Rad DC Protein Assay Kit (Pierce, Rockford, IL). Protein lysates subjected to electrophoresis in 10% polyacrylamide gels were separated at 120 V for 2 hours and transferred with 200 mA for 2 hours. Membranes were blocked with 5% milk for 60 min at 37 ºC. Membranes were incubated with primary antibodies against IL-6 (1:200), MCP-1 (1:200), TNF-α (1:100), L-ferritin (1:100) and H-ferritin (1:1000). The antibody against H-ferritin was purchased from Cell Signaling Technology (Danvers, MA). All the rest were purchased from Abcam (Cambridge, UK). They were incubated overnight at 4°C. Secondary antibodies were incubated at room temperature for 2 h. After washing with TBS-Tween

(10 min, three times), membranes were detected using the ECL Western blot detection system (Amersham Pharmacia, Deisenhofen, Germany). Sample loadings were normalized to β-actin expression.

Immunocytochemistry

Expression and localization of hepcidin and FPN1 in J774 macrophages were examined by immunofluorescent staining. J774 Macrophages with different treatments were cultured on glass coverslips and fixed in 4% paraformaldehyde. After a serial of washes with PBS, the slides were blocked in 5% goat serum in PBS for 30min. The primary antibodies for hepcidin (1:100, Abcam, Cambridge, UK) and Fpn1 (1:50, A&D, San Antonio, USA) were applied to the slides and incubated overnight at 4°C. Secondary anti-IgG specific antibodies, conjugated with Fluorescein Isothiocyante (FITC) and DAPI were used. J774 macrophages treated with normal goat IgG served as a negative control. The immunofluorescent staining of J774 macrophages was then observed on a fluorescent microscopy (Olympus, Tokyo, Japan).

Quantification of ROS production

Fluorescence measurement of ROS was performed with Flow Cytometer (FACSCalibur, BD, USA) equipped with a 488 nm argon laser using conventional methods. Briefly, J774 macrophages with different treatments were collected at indicated time points, and incubated with 2′,7′-Dichlorofluorescin diacetate (DCF-DA) from Sigma in 5% CO_2, 95% air at 37°C for 30 min followed by three washes with PBS . After re-suspending at a density of 1×10^6 cells/ml in PBS, the cells were measured immediately and data were analyzed with Cell Quest Pro (BD, New York, USA).

Detection of Apoptosis

Apoptosis was assessed by terminal deoxynucleotidyl transferase end-labelling (TUNEL, Calbiochem, EMD Bioscences, Germany) staining. Cells with TUNEL-positive nuclei as well as morphological features of apoptosis, such as cell shrinkage, nuclear pyknosis, chromatin condensation and nuclear fragmentation were counted as apoptotic cells. Nuclei were labeled with DAPI, and apoptotic cells were labeled with Methyl green. The apoptosis rate was expressed as the proportion of apoptotic cells to total number of cells in a given area. The number of TUNEL-positive cells was counted three times in randomly selected fields from each treatment.

ELISA

At the end of the second part of the *in vivo* study, blood was collected from the inferior vena cava before perfusion-fixation. The concentrations of hepcidin in serum were determined by ELISA (DRG instruments GmbH, Gemany) following the manufacturer's recommendations. The concentration of hepcidin in supernatant with different treatments was measured using the same method.

Quantification of Intracellular Lipids

The lipids of macrophages with different treatments were extracted with the Folch method**.** The organic phase was separated from protein and water phases with a solution of methanol and chloroform (volume 2:1). The solvent was completely evaporated in a stream of nitrogen and dissolved in a solution of methanol and chloroform (volume 2:1). The intracellular levels of TC, TG and LDL-C were measured by enzymatic assay.

Measurement of non-heme iron by Atomic absorption spectrometry

For non-heme iron, 20 mg left carotid plaque tissues were homogenized in 360μL of 6% TCA/0.5 mM EDTA and incubated at 90°C for 30min. After 0.7 ml of 0.5mM EDTA was added, samples were centrifuged at 13,000 × *g* for 10 min, and the supernatant was collected and measured by flame atomic absorption spectrometry with a Solar M-6 Atomic absorption spectrophotometer (Thermoelectric Company, USA).

Statistical analysis

All analyses were performed using SPSS 16.0 (SPSS Inc., Chicago, IL). Data were expressed as mean ± SE. An independent-samples t-test was used to compare continuous data for between-group differences and comparisons among groups involved the use of ANOVA with LSD post hoc test used for multiple comparisons. $P<0.05$ was considered statistically significant. All experiments were repeated for at least 3 times.

References

1. von der Thusen JH, van Berkel TJ, Biessen EA. Induction of rapid atherogenesis by perivascular carotid collar placement in apolipoprotein E-deficient and low-density lipoprotein receptor-deficient mice. *Circulation.* 2001;103:1164-1170.
2. Shiomi M, Ito T, Hirouchi Y, Enomoto M. Fibromuscular cap composition is important for the stability of established atherosclerotic plaques in mature WHHL rabbits treated with statins. *Atherosclerosis.* 2001;157:75-84.
3. Chung J, Haile DJ, Wessling-Resnick M. Copper-induced ferroportin-1 expression in J774 macrophages is associated with increased iron efflux. *Proc Natl Acad Sci U S A.* 2004;101:2700-2705.

4. Knutson MD, Vafa MR, Haile DJ, Wessling-Resnick M. Iron loading and erythrophagocytosis increase ferroportin 1 (FPN1) expression in J774 macrophages. *Blood.* 2003;102:4191-4197.

Supplemental Table. Effects of hepcidin on serum lipids and glucose levels

Parameters	**Ad-EGFP** (n=6)	**Ad-Hepcidin** (n=6)	**Ad-Hepcidin shRNA** (n=6)	*p*
TC (mmol/L)	7.12 ± 1.08	10.31 ± 0.86	8.87 ± 1.30	ns
TG (mmol/L)	0.28 ± 0.05	0.50 ± 0.11	0.49 ± 0.09	ns
LDL-C (mmol/L)	6.79 ± 0.35	7.92 ± 0.33	7.12 ± 1.34	ns
HDL-C (mmol/L)	3.66 ± 0.20	4.14 ± 0.10	3.54 ± 0.42	ns
Glucose (mmol/L)	3.24 ± 0.29	3.59 ± 0.28	3.61 ± 0.35	ns

TC, total cholesterol; TG, triglyceride; LDL-C, low density lipoprotein cholesterol; HDL-C, high density lipoprotein cholesterol; ns, no significant difference.

Legends for Supplemental Figures.

Supplemental Figure I. The endogenous expression of hepcidin in the carotid plaque of the model and control groups. A, Immunochemical staining of hepcidin (arrowheads) in the carotid plaques of the control and the model groups (the third row was an amplification of a section from the second row). **B,** Quantitative analysis of the results in supplemental Fig.1A. ***** $p<0.01$ vs. the control. (n=6 in each group). **C**, Hepcidin mRNA expression in the carotid plaques of the control and the model groups. ****** $p<0.001$ vs. the control. Four polls in each group and three mice as a poll.

Supplemental Figure II. Effects of ox-LDL treatment on erythrophagocytosed macrophages *in vitro*. Macrophages after erythrophagocytosis were treated with or without ox-LDL (50μg/ml) for 2 hours. A, Measurements of intracellular lipids in macrophages with different treatments. ** $p<0.001$ vs. control [phagocytosis (-) and ox-LDL (-)]; †† $p<0.001$ vs. phagocytosis or ox-LDL treatment alone (n=6). **B**, Protein expression levels of IL-6, MCP-1 and TNFα in macrophages with different treatments. **C,** Quantitative analysis of the results in supplemental Fig. 2B. * $p<0.01$ vs. control [phagocytosis (-) and ox-LDL (-)]; ** $p<0.001$ vs. control [phagocytosis (-) and ox-LDL (-)]; † $p<0.01$ vs. phagocytosis or ox-LDL treatment alone (n=6). **D,** mRNA expression levels of IL-6, MCP-1 and TNFα in macrophages with different treatments. * $p<0.01$ vs. control [phagocytosis (-) and ox-LDL (-)]; ** $p<0.001$ vs. control [phagocytosis (-) and ox-LDL (-)]; † $p<0.01$ vs. phagocytosis or ox-LDL treatment alone. (n=6). **E,** Measurements of ROS formation. MFI, mean fluorescence intensity. ***** $p<0.01$ vs. control [phagocytosis (-) and ox-LDL (-)]; ** $p<0.001$ vs. control [phagocytosis (-) and ox-LDL (-)]; † $p<0.01$ vs. ox-LDL treatment alone; # $p<0.05$ vs. phagocytosis treatment alone.

(n=6). **F,** Apoptosis assessment by TUNEL staining. Areas in green (arrowheads) indicated apoptotic cells and areas in blue showed nuclei. **G,** Quantitative analysis of the results in supplemental Fig. 2F. * $p<0.01$ vs. control [phagocytosis (-) and ox-LDL (-)]; ** $p<0.001$ vs. control [phagocytosis (-) and ox-LDL (-)]; † $p<0.01$ vs. phagocytosis or ox-LDL treatment alone (n=6).

Supplemental Figure III. Effects of hepcidin on ox-LDL-induced activation of macrophages without phagocytosis *in vitro*. Macrophages were treated with hepcidin (1μg/ml) and/or ox-LDL (50μg/ml) for 2 hours. **A,** Measurements of intracellular lipids in macrophages with different treatments. ** $p<0.001$ vs. control [hepcidin (-) and ox-LDL (-)] or hepcidin treatment alone. (n=6). **B,** Protein expression levels of IL-6, MCP-1 and TNF-α in macrophages with different treatments. **C,** Quantitative analysis of the results in supplemental Fig. 3B. * $p<0.01$ vs. control [hepcidin (-) and ox-LDL (-)] or hepcidin treatment alone; # $p<0.05$ vs. control [hepcidin (-) and ox-LDL (-)] or hepcidin treatment alone (n=6). **D,** mRNA expression levels of IL-6, MCP-1 and TNF-α in macrophages with different treatments. * $p<0.01$ vs. control [hepcidin (-) and ox-LDL (-)] or hepcidin treatment alone; ** $p<0.001$ vs. control [hepcidin (-) and ox-LDL (-)] or hepcidin treatment alone (n=6). **E,** Measurements of ROS formation. MFI, mean fluorescence intensity. * $p<0.01$ vs. control [hepcidin (-) and ox-LDL (-)] or hepcidin treatment alone (n=6). **F,** Apoptosis assessment by TUNEL staining. Areas in green (arrowheads) indicated apoptotic cells and areas in blue depicted nuclei. **G,** Quantitative analysis of the results in supplemental Fig. 3F. ** $p<0.001$ vs. control [hepcidin (-) and ox-LDL (-)] or hepcidin treatment alone (n=6).

Supplemental Figure IV. Effects of iron chelators on the activation of macrophages with or without phagocytosis *in vitro*. Macrophages with or without erythrophagocytosis were treated with or without iron chelator [DFO (200 μM) + BPDL (100 μM)] for 2 hours. DFO, deferoxamine； BPDL, 2,2’-bipyridyl. **A,** Protein expression levels of H-ferritin and L-ferritin in macrophages with different treatments. **B,** Quantitative analysis of the results in supplemental Fig. 4A. * p<0.01 vs. control [phagocytosis (-) and iron chelator(-)], # p<0.05 vs. control [phagocytosis (-) and iron chelator(-)], † p<0.01 vs. phagocytosis treatment alone (n=6). **C**, Measurements of intracellular lipids in macrophages with different treatments. ** p<0.001 vs. control [phagocytosis (-), ox-LDL (-) and iron chelator (-)], †† p<0.001 vs. phagocytosis treatment alone (n=6), † p<0.01 vs. iron chelator (-) (n=6). **D,** Protein expression levels of IL-6, MCP-1 and TNFα in macrophages with different treatments. **E,** Quantitative analysis of the results in supplemental Fig. 4D. * p<0.01 vs. control [phagocytosis (-) and iron chelator (-)], # p<0.05 vs. control [phagocytosis (-) and iron chelator (-)], † p<0.01 vs. phagocytosis treatment alone (n=6). **F,** mRNA expression levels of IL-6, MCP-1 and TNF-α in macrophages with different treatments. * p<0.01 vs. control [phagocytosis (-) and iron chelator(-)], † p<0.01 vs. phagocytosis treatment alone (n=6). **G,** Measurements of ROS formation. MFI, Mean Fluorescence Intensity. * p<0.01 vs. control [phagocytosis (-) and iron chelator(-)], † p<0.01 vs. phagocytosis treatment alone (n=6). **H,** Apoptosis assessment by TUNEL staining. Areas in green (arrowheads) signified apoptotic cells and areas in blue depicted nuclei. **I,** Quantitative analysis of the results in supplemental Fig. 4H. * p<0.01 vs. control [phagocytosis (-) and iron chelator(-)], † p<0.01 vs. phagocytosis treatment alone (n=6).

Supplemental Figure Ⅴ. Erythrophagocytosis-induced expression of FPN1 and ferritin in macrophages and the effect of hepcidin on FPN1 expression in erythrophagocytosed macrophages *in vitro*. A, mRNA expression levels of FPN1, H-ferritin and L-ferritin in macrophages at different time points after erythrophagocytosis (n=6). **B**, Immunocytochemical staining of FPN1 expression. Areas in red (arrowheads) displayed staining for FPN1 and areas in blue showed nuclei. **C,** Quantitative analysis of the results in supplemental Fig. 5B. * p<0.01 vs. macrophage without phagocytosis; † p<0.01 vs. phgaocytosed macrophage without hepcidin treatment (n=6).

Supplemental Figure Ⅵ. The comparison of inflammation, apoptosis and ROS formation between the control and model groups. A, Immunochemical staining of IL-6, MCP-1, TNFα and MMP-2 in the carotid plaques of the control and the model groups. Arrowheads indicated positive staining areas in brown. **B,** Quantitative analysis of IL-6 protein expression in supplemental Fig. 6A. ** p<0.001 vs. control group (n=6). **C,** Quantitative analysis of MCP-1 protein expression in supplemental Fig.6A. ** p<0.001 vs. control group (n=6). **D,** Quantitative analysis of TNFα protein expression in supplemental Fig. 6A. ** p<0.001 vs. control group (n=6). **E,** Quantitative analysis of MMP-2 protein expression in supplemental Fig. 6A. ** p<0.001 vs. control group (n=6). **F,** mRNA expression of IL-6, MCP-1, TNFα and MMP-2 in the carotid plaques of the control and the model groups. ** p<0.001 vs. control group (n=6). **G,** Dihydroethidium (DHE) staining of ROS in the carotid plaques of the control and the model groups. Arrowheads indicated the positive areas. **H,** Quantitative analysis of the Florescence Intensity in supplemental Fig. 6G. ** p<0.001 vs. control group (n=6). **I,** Apoptosis assessment by TUNEL staining. Arrowheads indicated the apoptotic cells. **J,**

Quantitative analysis of the results in supplemental Fig. 6I. ** p<0.001 vs. control group (n=6).

Supplemental Figure VII. Effects of hepcidin on ox-LDL-induced activation of primary macrophages in the setting of erythrophagocytosis. A, The effect of hepcidin on ox-LDL-induced lipid accumulation in erythrophagocytosed primary macrophages, * p<0.01 vs.control [ox-LDL (-) and hepcidin (-)], † p<0.01 vs. ox-LDL treatment alone. **B,** The effect of hepcidin on ox-LDL-induced protein expression of IL-6, MCP-1 and TNFα in erythrophagocytosed primary macrophages. **C,** Quantitative analysis of the results in supplemental Fig. 7B. * p<0.01 vs. control [ox-LDL (-) and hepcidin (-)], # p<0.05 vs. control [ox-LDL (-) and hepcidin (-)], † p<0.01 vs. hepcidin or ox-LDL treatment alone, § p<0.05 vs.hepcidin or ox-LDL treatment alone. **D,** The effect of hepcidin on ox-LDL-induced mRNA expression of IL-6, MCP-1 and TNFα in erythrophagocytosed primary macrophages. * p<0.01 vs. control [ox-LDL (-) and hepcidin (-)], † p<0.01 vs. hepcidin or ox-LDL treatment alone. **E,** The effect of hepcidin on ox-LDL-induced ROS formation in erythrophagocytosed primary macrophages. MFI, mean fluorescence intensity. * p<0.01 vs. control [ox-LDL (-) and hepcidin (-)]; # p<0.05 vs. control [ox-LDL (-) and hepcidin (-)]; † p<0.01 vs. hepcidin or ox-LDL treatment alone. **F,** The effect of hepcidin on ox-LDL-induced apoptosis in erythrophagocytosed primary macrophages. Areas in green (arrowheads) indicated apoptotic cells and areas in blue depicted nuclei. **G,** Quantification of the TUNEL staining in supplemental Fig. 7F. * p<0.01 vs. control [ox-LDL (-) and hepcidin (-)]; † p<0.01 vs. hepcidin or ox-LDL treatment alone. All the results were representatives of 6 independent experiments.

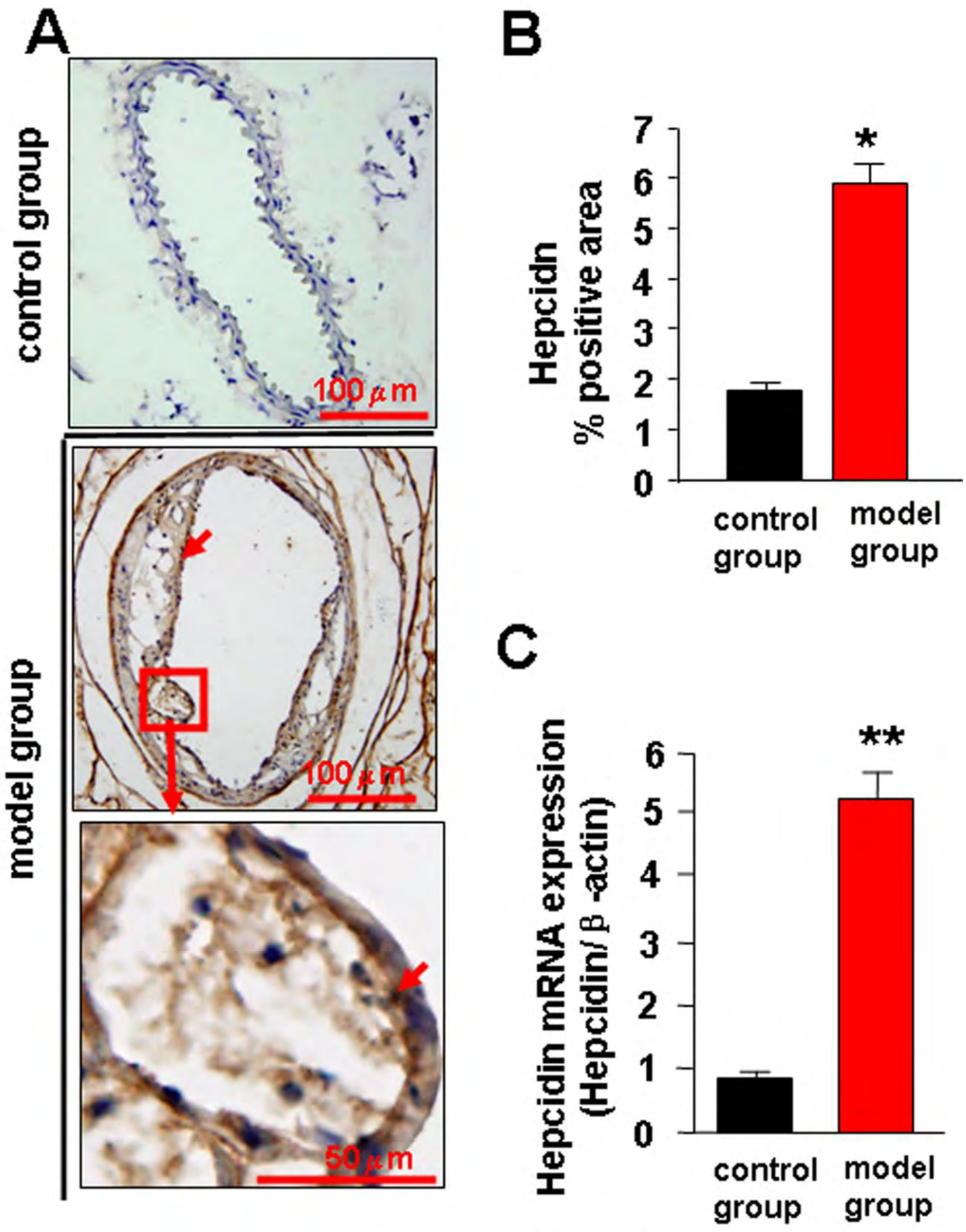

Suppl Figure I

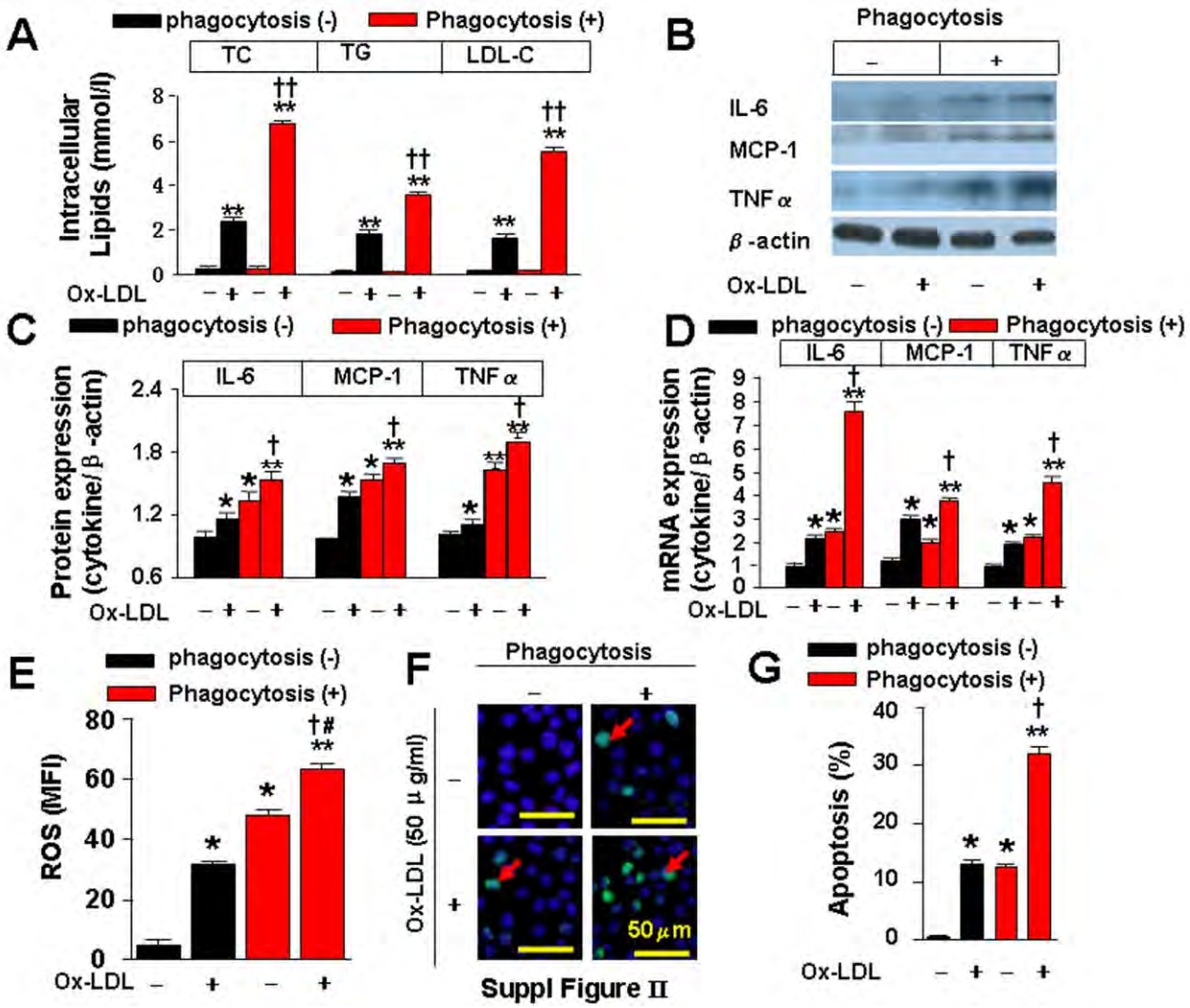

Suppl Figure II

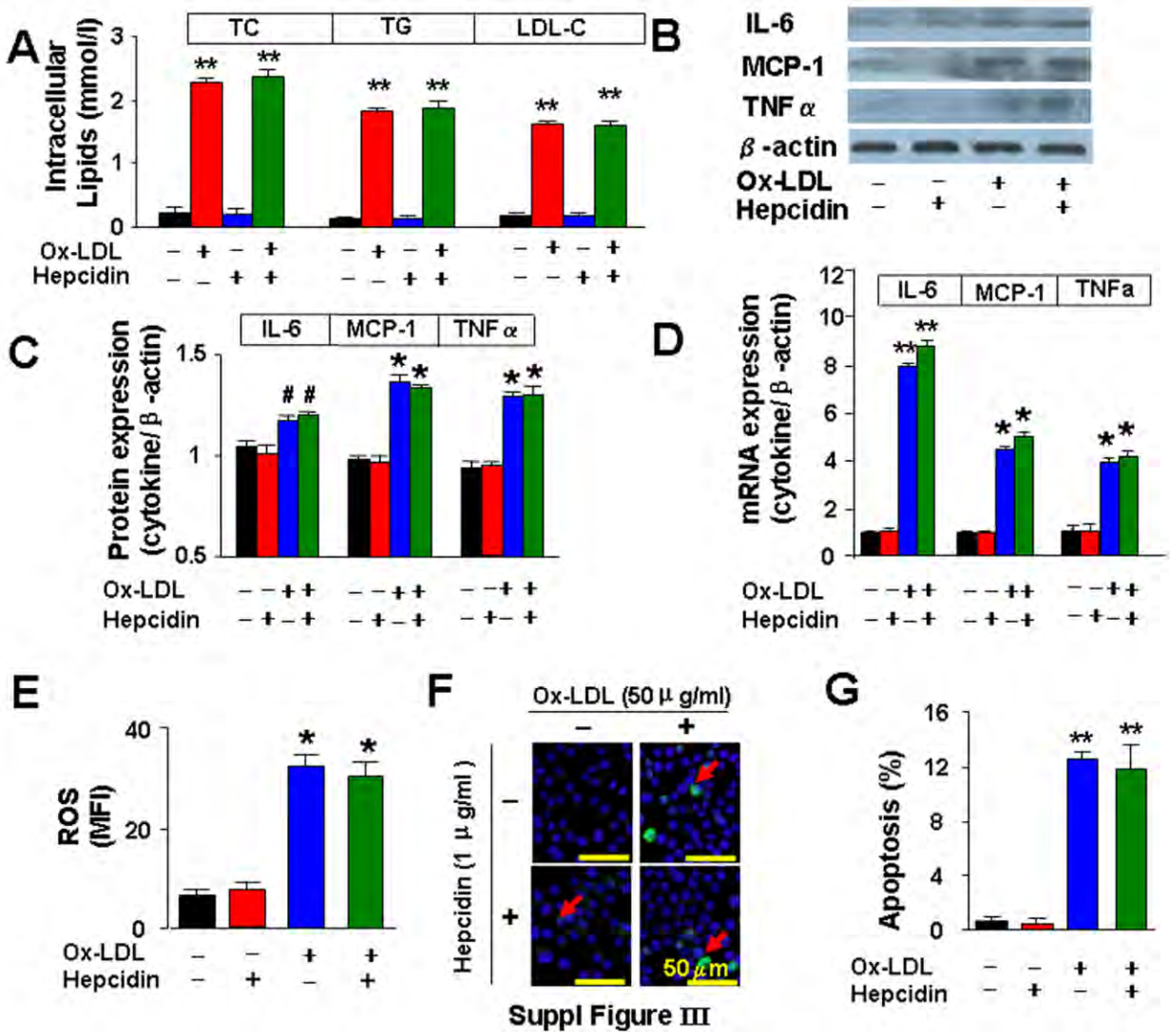

Suppl Figure III

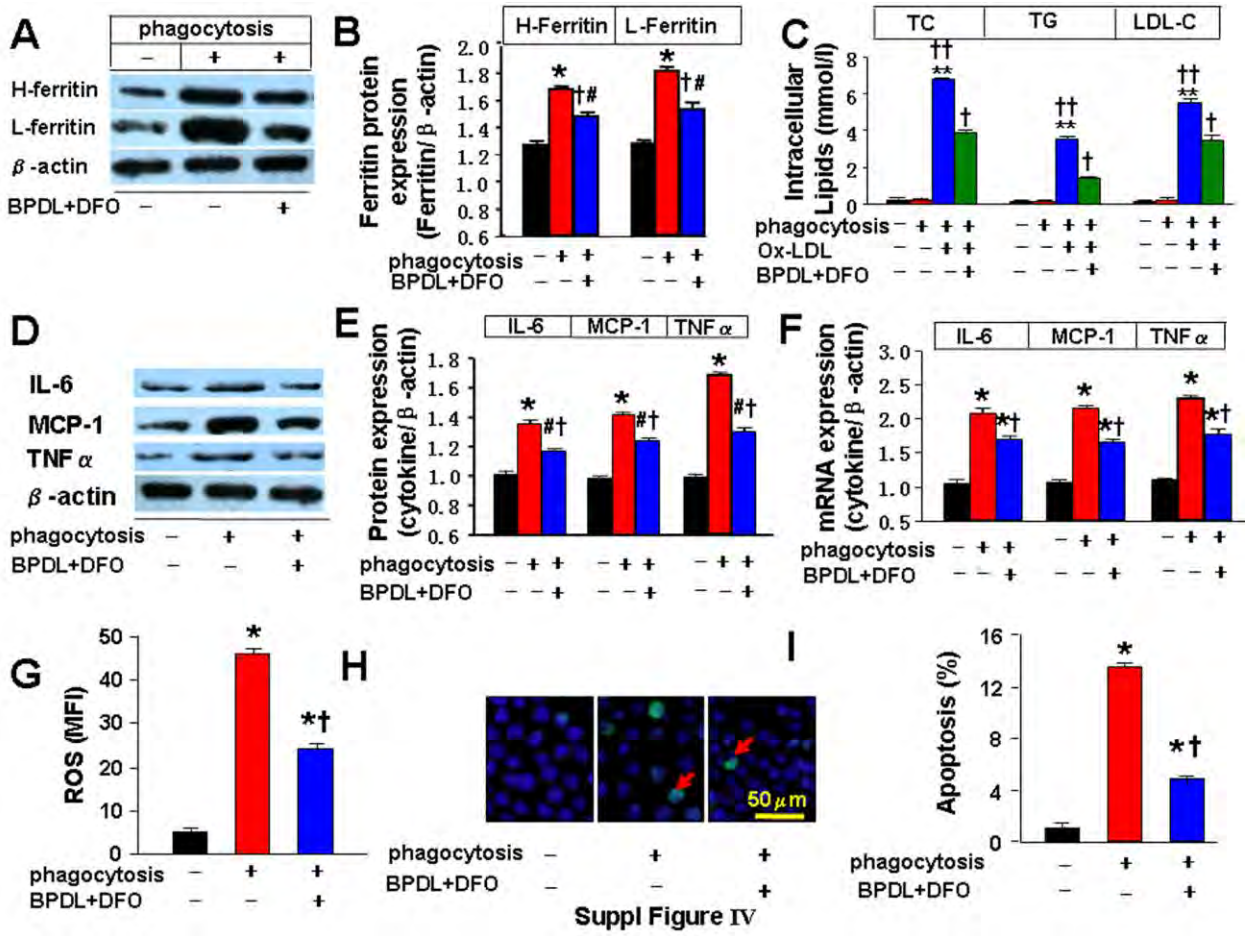

Suppl Figure IV

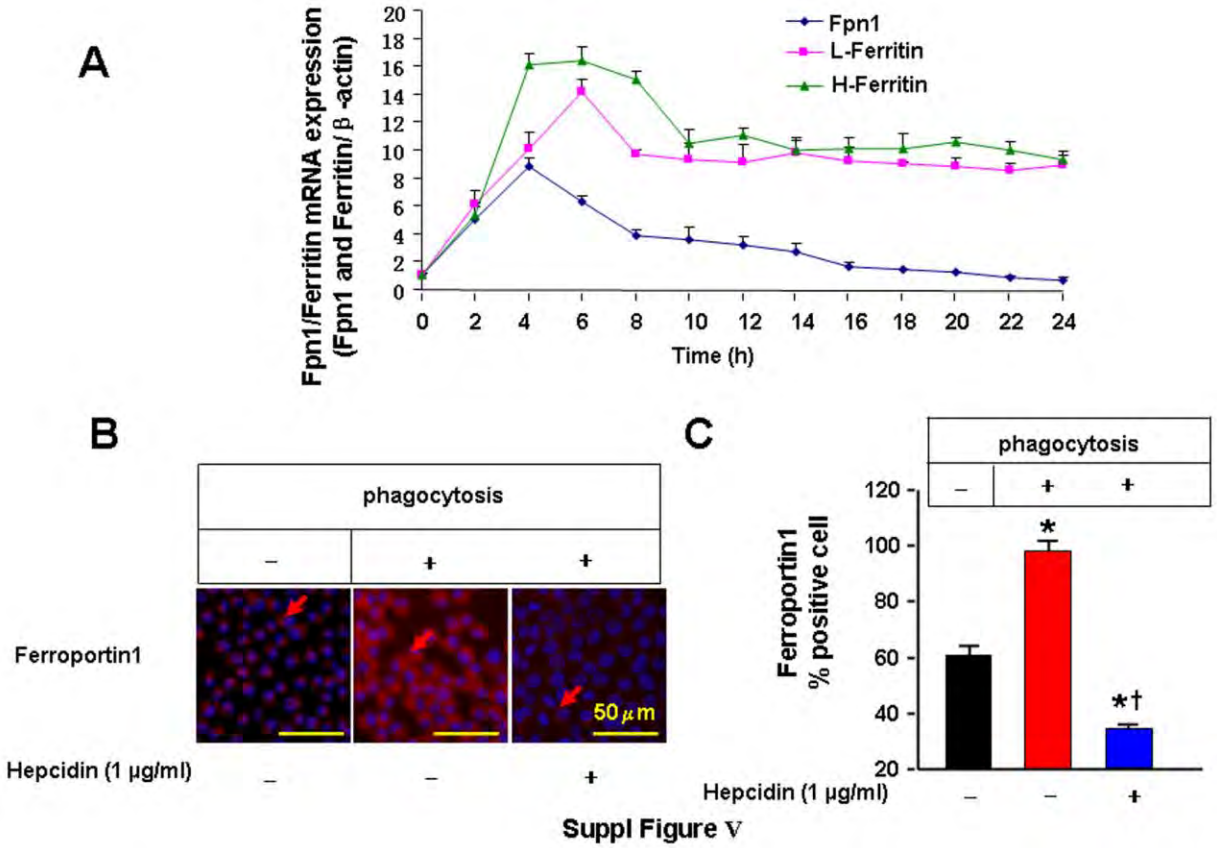

Suppl Figure V

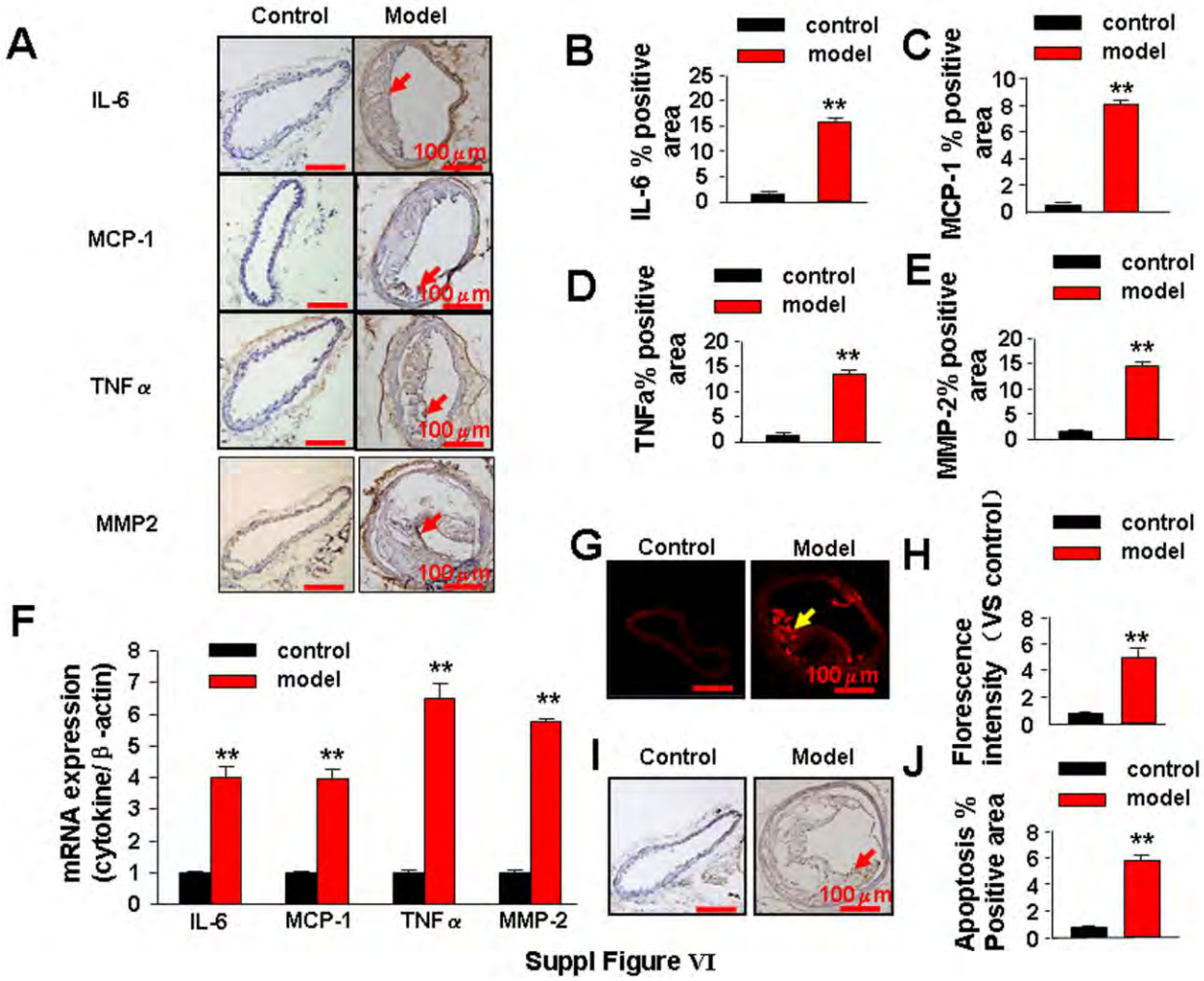

Suppl Figure VI

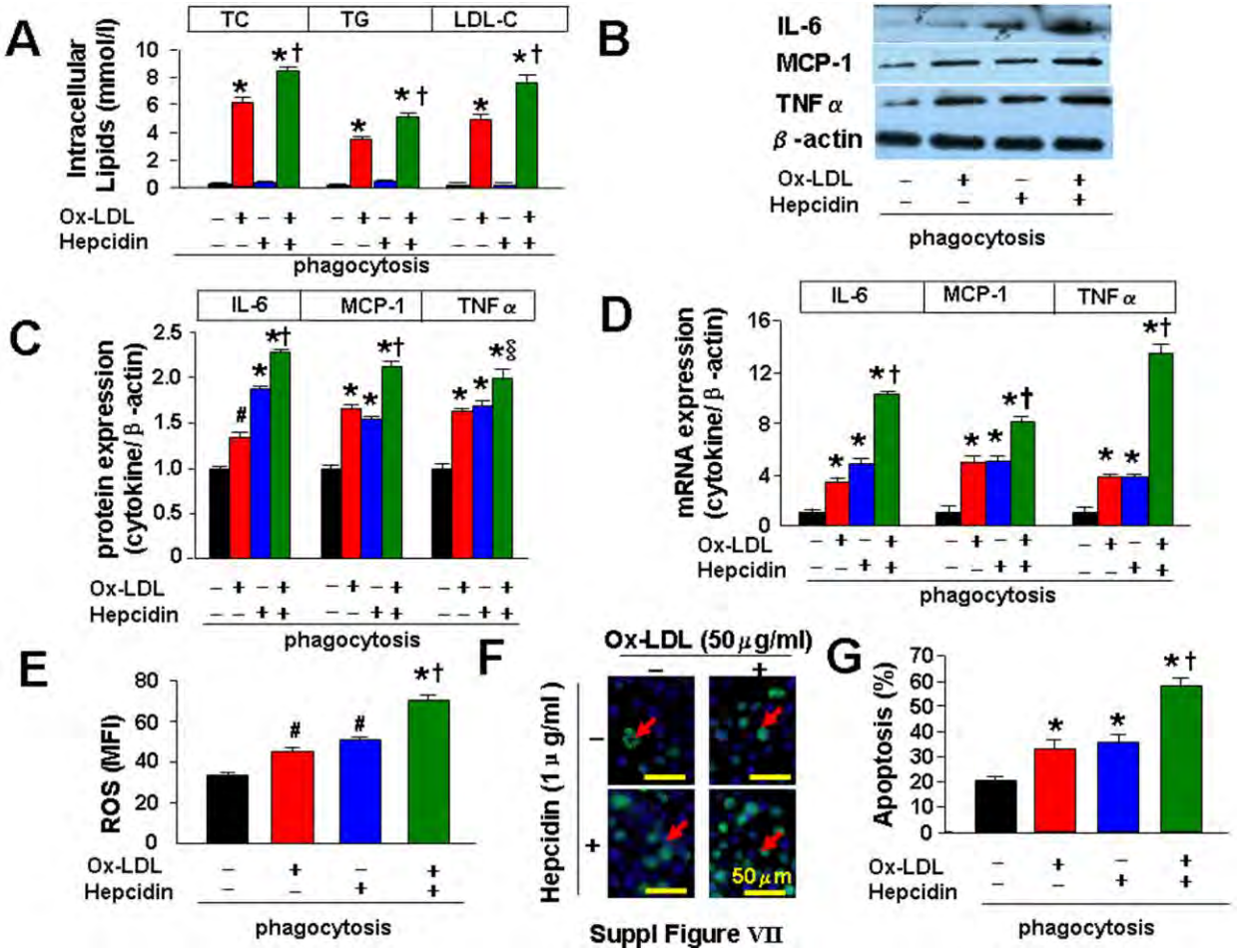

Suppl Figure VII